Transportation Research Part D 95 (2021) 102843

Contents lists available at ScienceDirect

Transportation Research Part D

journal homepage: www.elsevier.com/locate/trd

Development of heavy-duty vehicle representative driving cycles via decision tree regression

Chen Zhang [a,*], Andrew Kotz [a], Kenneth Kelly [a], Luke Rippelmeyer [b]

[a] National Renewable Energy Laboratory, United States
[b] Toyota Motor North America, United States

ARTICLE INFO

Keywords:
Heavy-duty vehicle
Powertrain electrification
Decision tree regression
Representative driving cycle
On-road data

ABSTRACT

Previously, researchers who developed representative driving cycles mainly focused on light-duty vehicles and only considered vehicle speed and related derivations. In this paper, we propose a novel approach to develop representative cycles for heavy-duty vehicles. By implementing decision tree regression (DTR) to the Fleet DNA on-road vehicle data, a broader set of metrics, such as engine power and fuel consumption, can be used for more robust cycle development. Additionally, the influence of each metric on the regression target is also accounted for by a weighted number derived through the DTR to enhance the representativenss of the developed cycle. As case studies, we applied the proposed method to five heavy-duty vocations (drayage, long haul, regional haul, local delivery, and transit bus) and derived the most representative cycle, as well as four extreme cycles (maximal energy consumption, maximal power-weighted work, maximal fraction of high speed, and minimal fuel economy) to advance the related alternative powertrain design.

1. Introduction

Almost 70% of petroleum consumed in the United States is consumed by the transportation sector. This accounts for 28% of national energy and more than 30% of greenhouse gas emissions (Davis and Boundy, 2019; EPA, 2020). Within the transportation sector, heavy-duty vehicles (HDVs) consume 15% of U.S. petroleum (or 19.8%, if off-highway HDVs are included), second only to light-duty vehicles (Davis and Boundy, 2020). However, the U.S. Energy Information Administration has projected that HDV fleet fuel consumption will grow twice as fast as that of the light-duty fleet (EIA, 2020). If this projection comes to reality, improving fuel economy and thus reducing the related CO_2 emissions for HDVs will become increasingly important.

New technologies are incrementally incorporated into HDVs to help improve vehicle efficiency and reduce environmental impact (EPA, 2020; CARB, 2021). Among these technologies, powertrain electrification, realized by battery or fuel cell, has attracted wide attention from the public. Referring to battery electric vehicles, Mercedes-Benz Trucks became one of the first manufacturer worldwide to present an electric heavy tuck, eActros, in 2016 (Daimler, 2021). Two years later, Volvo Trucks also introduced its first all-electric truck—the Volvo FL Electric—for urban distribution and refuse operation (AB Volvo, 2018). Tesla, a leader in the light-duty electric vehicle market, also unveiled its first heavy-duty electric truck—the Tesla Semi—in November 2017 (Tesla, 2021). On the other hand, due to H_2's energy density and zero-carbon emission (Zhang and Sun, 2017), many manufacturers have also evaluated fuel cell performance on HDVs. In 2018, Toyota debuted its Beta model fuel-cell-powered semi-truck in Michigan, which extended the driving

* Corresponding author.
E-mail address: chen.zhang@nrel.gov (C. Zhang).

https://doi.org/10.1016/j.trd.2021.102843

Available online 5 May 2021

range by 25% and increased power output by 10% compared to its predecessor (O'Dell, 2018). Similarly, Hyundai Motor announced that it will produce 1,000 fuel cell electric trucks for the Swiss commercial vehicle market from 2019 through 2023 (Hyundai, 2018)). Since 2000, the National Renewable Energy Laboratory (NREL) has made a remarkable effort to record the status and progress of fuel cell transit buses in the United States. An NREL report from 2018 summarizes the progress of fuel cell electric bus development in the United States and discusses the achievements and challenges of introducing fuel cell propulsion in transit (Eudy and Post, 2018).

Because numerous vocations exist among HDVs (e.g., long-haul truck, local delivery truck, transit bus), one big issue related to electrification—whether battery or fuel cell—is how to size the powertrain system to meet the requirements of a specific vocation. A limited system may not satisfy all the performance requirements, whereas a redundant system increases a vehicle's market price and postpones the corresponding technology penetration. To optimally design the powertrain, one critical step is characterizing the driving behavior of the heavy-duty (HD) vocation under consideration. Such a characterization includes not only the distribution of significant performance metrics (e.g., average vehicle speed, peak power, energy consumption on a daily basis), but also representative and extreme driving cycles from the real world. Previously, developing representative driving cycles involved generating micro-trips based on multiple segmentation methods and then randomly recombining them to match the specific trip metrics (Andre, 1996). One older example is the unified cycle (the LA92 driving cycle), proposed by the California Air Resources Board and developed using data collected in Los Angeles in 1992 (Austin et al., 1993). Since then, Kamble et al. have utilized similar methods to develop a representative driving cycle for Pune, India, which considers five metrics in the time–space profile: average speed and percentage of acceleration, deceleration, idle, and cruise (Kamble et al., 2009). In Canada, Seers et al. developed two driving cycles for suburban roadwork vehicles and airport utility vehicles, respectively (Seers et al., 2015). It should be noted that Seers et al. considered not only specific metrics like average speed, maximum speed, and positive kinetic energy, but also the speed-acceleration frequency distribution (SAFD) matrix, while selecting the final cycle from the micro-trip pools. Ho et al. developed a Singapore driving cycle for passenger cars through this micro-trip approach integrated with a consideration of road type and time period (Ho et al., 2014). Unlike the aforementioned examples, Gunther et al. developed a dynamic driving cycle for bus application in Germany (Gunther et al., 2017), specifically selecting seven parameters randomly through Weibull or lognormal distributions and then constructing a variable micro-trip with the representativeness. Other similar works include (Hung et al., 2007; Esteves-Booth et al., 2001; Tzirakis et al., 2006; Amirjamshidi and Roorda, 2015).

Recently, many researchers have considered vehicle operation as a first order Markov process and applied Markov chain theory to design driving cycles. The basic idea of this method is to claim that the next speed and acceleration state of a vehicle depends only on the current state rather than the previous ones. In this way, by collecting real-world data and deriving the corresponding state-transition matrix, the driving cycle can be eventually determined after applying the maximum likelihood estimation (Lin and Niemeier, 2002), Monte Carlo simulation (Shi et al., 2016), or simulated annealing optimization algorithm (Sun et al., 2019). Machine-learning-based methods are also involved in the development of driving cycles. K-mean clustering (Duran et al., 2018; Fotouhi and Montazeri-Gh, 2013), support vector machine (Zhao et al., 2018), and neural network (Brady and O'Mahony, 2016) have all been applied recently. However, the applications of these machine-learning approaches still focus on how to cluster the micro-trips into different groups according to speed or acceleration metrics and then select the corresponding micro-trip from each cluster.

One issue from the previous work on cycle development is that the trip statistic metrics mainly consist of speed, acceleration, and other related parameters. As (Shi et al., 2016) mentions, if one only considers the vehicle speed and acceleration profile, some other important information related to HDV operation may be missed, thus undermining the representativeness of the developed driving cycles. Such information includes payload, road grade, gear selection, engine torque, fuel consumption and so on. All of them would affect actual vehicle driving behavior and related powertrain performance requirements, while the speed and acceleration cannot represent them thoroughly. For example, the energy consumption from an empty long-haul truck cruising at 105 km/h (64 mph) is much less than a full-load truck driving at the same speed. However, this difference cannot be reflected by only taking the speed (identical to each other) into consideration.

Traditional approaches that randomly combine the generated micro-trips are not appropriate for heavy-duty vehicles since the engine power and torque are likely to be discontinuous from at the micro-trip interface. For example, while the vehicle speed at the end of one micro-trip is zero, the engine may be shut off - producing zero output power, or it may be idling for low load work or accessory loads. Even in the idle condition, the engine output power from one micro-trip to the next may still be discontinuous based on accessory loads, emission control strategies and thermal response. Further, recombining micro-trips from different times can produce inaccurate or discontinuous mass and grade profiles. In addition, whether the engine power and consumption can be recognized as a first-order Markov process is still an open question. Given these observations, we suggest that continuous driving data derived from extensive on-road database is a better option to design representative cycles.

In this paper, we propose a novel approach to develop representative driving cycles for HDVs. The essence of this approach is to implement state-of-the-art decision tree regression (DTR) into the Fleet DNA data set (NREL, 2021). The advantages of this approach include the following:

- Not only vehicle speed and acceleration, but also other metrics (e.g., engine torque, fuel economy) can be extracted from the Fleet DNA data set and provide more practical insights to develop the representative cycles.
- A regression target can be assigned in the DTR, which determines the objective of the representativeness. In this study, energy consumption per driving kilometer was set as the target.
- The influence of each metric on the regression target may be different. Using DTR, a weighted number was calculated for each metric, which accounts for such various influences. In this way, the highest representativeness was guaranteed in the developed cycle.

- This approach can be easily extended by taking more metrics into consideration or assigning other regression targets per the motivation and requirement of other projects. Additionally, if data from other countries are available, this approach can be leveraged to design related representative cycles.

We selected five different vocations in the Class 8 heavy-duty segment as case studies to demonstrate the effectiveness of this approach. We investigated Class 8 vocations first because they have the highest fuel consumption in the HD vehicle market (EPA, 2020). The vocations investigated in this study are long-haul trucks, regional-haul trucks, drayage trucks, local delivery trucks, and transit buses. Beyond the most representative daily driving cycle, other daily trips characterized by maximal energy consumption, minimal fuel economy, highest fraction of high speed (>88 km/h), and maximal power-weighted work were also determined for each vocation. The latter four daily trips can be assigned as extreme driving cycles, which are also valuable for the design of the electrical power system. It should be noted that in addition to the system design, the developed driving cycles can also be input into specific downstream applications to build up the national-scale fuel consumption and emissions inventory. One possible example of these downstream applications is the Vehicle Energy Consumption Calculation Tool (VECTO), a new simulation tool developed by the European Commission aimed at determining the CO_2 emissions and fuel consumption from HDVs (EU Commission, 2021).

In the rest of the paper, we first present an introduction of the data source, Fleet DNA. Next, we describe the detailed approach to determine representative driving cycles from the on-road data and the machine-learning analytical method—decision tree regression. Afterwards, five representative driving cycles in each of the five vocations will be illustrated with details. Finally, the paper concludes by summarizing the main results of this study and potential future work.

2. Data sources – Fleet DNA

The Fleet DNA clearinghouse of commercial fleet transportation data was developed by the Commercial Vehicle Technologies Team at NREL by collecting and storing medium- and heavy-duty vehicle data from multiple U.S. Department of Energy projects and other industry activities (NREL, 2021). Fleet DNA consists of over 2,700 vehicles with more than 18 million driven kilometers spanning a variety of vocations, vehicle types, and locations within the United States (Fig. 1). Such extensive data are necessary to capture the wide range of vehicle operations resulting from different geographies and fleet applications demonstrated by medium- and heavy-duty vehicles. As a result, this database is leveraged to help vehicle manufacturers and automobile developers optimize vehicle design, to help fleet managers choose advanced technologies for their fleets, and to help policymakers establish regulatory and certification standards based on real-world situations. Fleet DNA is widely used to calculate in-use fuel economy, perform drive-cycle characterization, and analyze system-level duty cycles, which can be complemented with chassis dynamometer emissions and efficiency tests. These studies provide feedback to stakeholders such as fleets, technology providers, researchers, and government agencies, helping to inform and provide insight on the performance of advanced technology and fuels operating under real-world conditions.

Data include not only GPS and route data such as latitude/longitude, vehicle speed, road grade, and other environmental conditions, but also engine controller area network (CAN) bus data via the SAE J1939 protocol. Such data have the fidelity to capture instantaneous engine speed, torque, fuel consumption, emissions production, coolant temperatures, and catalyst operation, and data are typically collected and stored at a 1-Hz or greater frequency.

In this study, five vocations from the heavy-duty market are of greatest interest, including long haul, drayage, regional haul, local delivery, and mass transit. A list of the Fleet DNA data used in this study is shown in Table 1, which includes the number of vehicles, number of vehicle days, and the corresponding driving mileage for each vocation.

Raw data was preprocessed to accurately characterize vehicle performance and eliminate erroneous signal, which include:

1. *Remove the first and last days of data*: Because the data logger was usually installed and uninstalled on the first and last days of project, these two days were eliminated to avoid counting incomplete or unrepresentative operation.
2. *Remove daily trips with distance less than 1.6 km (1 mile)*: This filter can eliminate any short trips that occur other than normal operation, like filling the gas or maintenance service.
3. *Filter out unrealistic values*: Some vehicle CAN bus signals will report meaningless default values (usually this is the "FF" or highest value in hex notation) prior to powering down or before a signal becomes active, which can cause unrealistic values such as the engine speed exceeding 8,000 rpm or fuel rate over 3,000 L per minute. Signal-specific filters are utilized in this step to remove such data points.
4. *Apply the zero-speed filter*: Zero-speed drift appears when the engine is stopped for a prolonged period while the vehicle key is still on. During this time, the installed data logger may record a nonzero engine speed, resulting in a sudden signal jump. In order to remove this error, we applied a data filter that examines the second-by-second engine speed data and removes all the single nonzero engine speeds. This simple filter improved the continuity of the raw data significantly.
5. *Fill time gaps greater than 20 min after an engine start*: Often, there are some "gaps" in time stamps between data points caused by pauses in the recording of the data logger while saving a log file to memory. However, it is also possible that a data logger will shut off prior to recording a zero for engine speed, and it is unclear from the data if the engine turned off or not. As a result, a gap-filling algorithm was used to infer engine stops and starts that may have been missed. In this way, any time gap over 20 min is assumed as an engine-off event.

For more clarification, Fig. 2 below shows the corresponding flow chart that describing the above data preprocessing.

Fig. 1. Map showing freight volumes (red) along major U.S. roadways and Fleet DNA data coverage (green) along those routes, as well as the involved vehicle vocations. (For interpretation of the references to colour in this figure legend, the reader is referred to the web version of this article.)

3. Approach

The first step to characterize vehicle driving behavior is to extract the statistical information from each HD vocation. Statistical information for one vocation includes detailed illustration of all vehicle speed, engine torque, and engine power, as well as the bin distributions of daily trip-based brake energy, driving mileage, fuel consumption, fuel economy, average speed, and fraction of high driving speed.

Given this information, we then identified the following drive cycles of greatest interest to characterize a specific vocation by considering five driving cycle types consisting of both extreme driving conditions and the most representative operation:

1. Daily trip with maximal energy consumption – informs the energy storage requirement
2. Daily trip with maximal power-weighted work – informs the high-power requirement
3. Daily trip with maximal time duration at high speed (over 88 km/h or 55 mph) – informs high speed operation, which produces the most aerodynamical drag force.
4. Daily trip with minimal fuel economy – informs the low efficiency operation of diesel engine and indicates the opportunities for alternative powertrain system.
5. Daily trip that is most representative – informs the typical energy use for the vocation.

The first four cycles are derived directly via the statistical information but determining the most representative driving cycle is more challenging. Many different metrics exist to explain a drive cycle, but depending on the objective, whether it be representative fuel economy or total work, these values can vary in both magnitude and impact on the target metric. The efforts described in this work use machine learning to develop a method for comparing values of different magnitude and influence on the target objective, ensuring parameters are weighted and captured based on importance to identify a vehicle duty cycle.

Decision tree regression is a machine-learning approach applied to the statistics in each vocation and vehicle daily trip that is used to identify the influence each parameter has on the target metric (Rokach and Maimon, 2008). DTR is a predictive modeling approach used in statistics and data mining. In general, DTR splits the data based by data entropy or explanation of variance and then performs a local linear regression on the new subsets of data. Each time the data splits, the number of subsets doubles, giving the "tree" a new

Table 1
Statistics of vehicle data segmented by vocations in Fleet DNA.

Vocation	# of Vehicles	# of Vehicle Days	Total Mileage (km)
Drayage	31	569	123,600
Long Haul	11	179	226,217
Regional Haul	62	772	543,641
Local Delivery	24	404	86,397
Transit Bus	9	147	34,301
Total	137	2,071	1,014,158

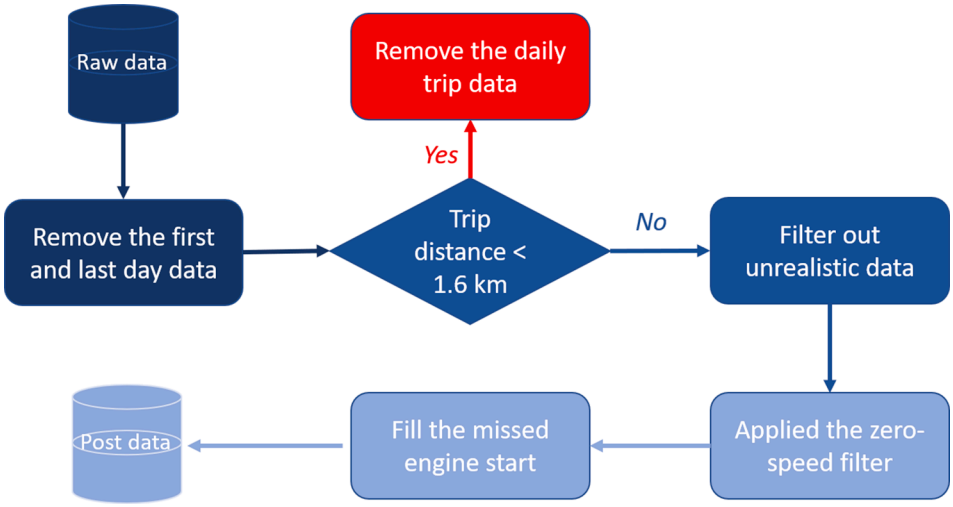

Fig. 2. Flow chart representing the data preprocessing.

depth. Success of the DTR is based on the mean square error (MSE) between predicted and actual values. The outputs of the DTR include parameter weight and correlation, where those parameters with a higher influence on the prescribed targets have a higher weight.

To use the DTR algorithm, both a list of metrics and the regression targets must first be determined. In this study, the regression target is set as the flywheel energy production per mile (kWh/mi) from the engine for each daily trip. Based on the outcome of this analysis, corresponding metrics including power parameters, vehicle parameters, and route parameters are proposed (Table 2). The power parameters are designed to reflect the energy consumption of each daily trip, which includes fuel economy and brake-specific fuel consumption. Vehicle parameters are designed to describe vehicle performance (e.g., total work, percentage time in idle mode, power-weighted work). The last data set—route parameters—includes essential information, such as stops per mile, average, maximal and standard deviation of speed, trip distance, aerodynamic velocity, and kinetic intensity.

Most of the parameters in Table 2 are self-explained, while some definitions were required for characteristic acceleration, aerodynamic velocity, kinetic intensity, and power-weighted work. Characteristic acceleration, aerodynamic velocity and kinetic intensity are all new cycle metric, introduce by NREL (O'Keefe et al., 2007). Specifically, the characteristic acceleration is a mass- and distance-specific measure of energy put forth to accelerate or raise a vehicle. The following equation shows the derivation of this term $\tilde{a}$:

Table 2
Daily trip metrics and DTR output – drayage.

Power Parameters	**Weight**
Fuel economy	83.71%
Brake-specific fuel consumption	16.29%
Vehicle Parameters	**Weight**
Percentage of time in idle operation	41.57%
Total work produced by engine	23.41%
Total fuel consumption	23.11%
Power-weighted work	11.91%
Route Parameters	**Weight**
Percentage of time while vehicle is zero speed	45.95%
Average driving speed	16.94%
Characteristic acceleration	15.53%
Percent of distance less than 5 miles per hour (mph) (8 km/h)	6.95%
Trip distance	4.67%
Aerodynamic velocity	4.07%
Average speed	3.91%
Standard deviation driving speed	1.15%
Maximum speed	0.68%
Number of vehicles stops per mile	0.07%
Percent of distance 5–15 mph (8–24 km/h)	0.06%
Percent of distance greater than 55 mph (88 km/h)	0.00%
Kinetic intensity	0.00%

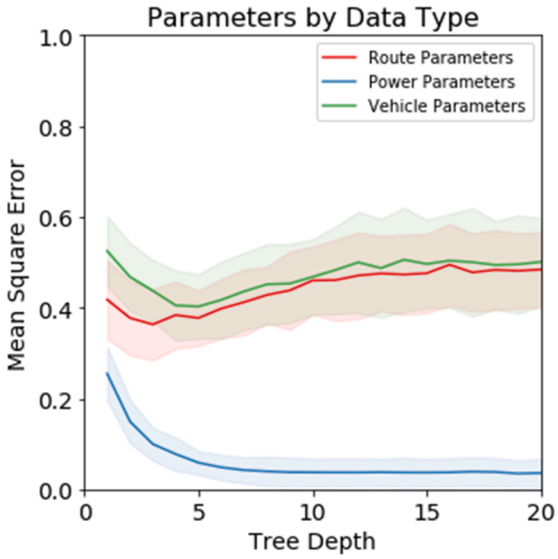

Fig. 3. Mean square error vs. tree depth for each parameter set in drayage.

$$\widetilde{a} = \frac{\sum_{j=1}^{N-1} positive\left(\frac{1}{2}\left(v_{j+1}^2 - v_j^2\right) + g \cdot \left(h_{j+1} - h_j\right)\right)}{D} \tag{1}$$

where D is the trip distance, v_j is the instantaneously velocity, h_j is the instantaneously elevation, and g is the gravity constant.

The aerodynamic speed shows the ratio of the overall average cubic speed to the average speed. It is directly linked to the impact of aerodynamics on vehicle fuel usage. The corresponding derivation is shown below:

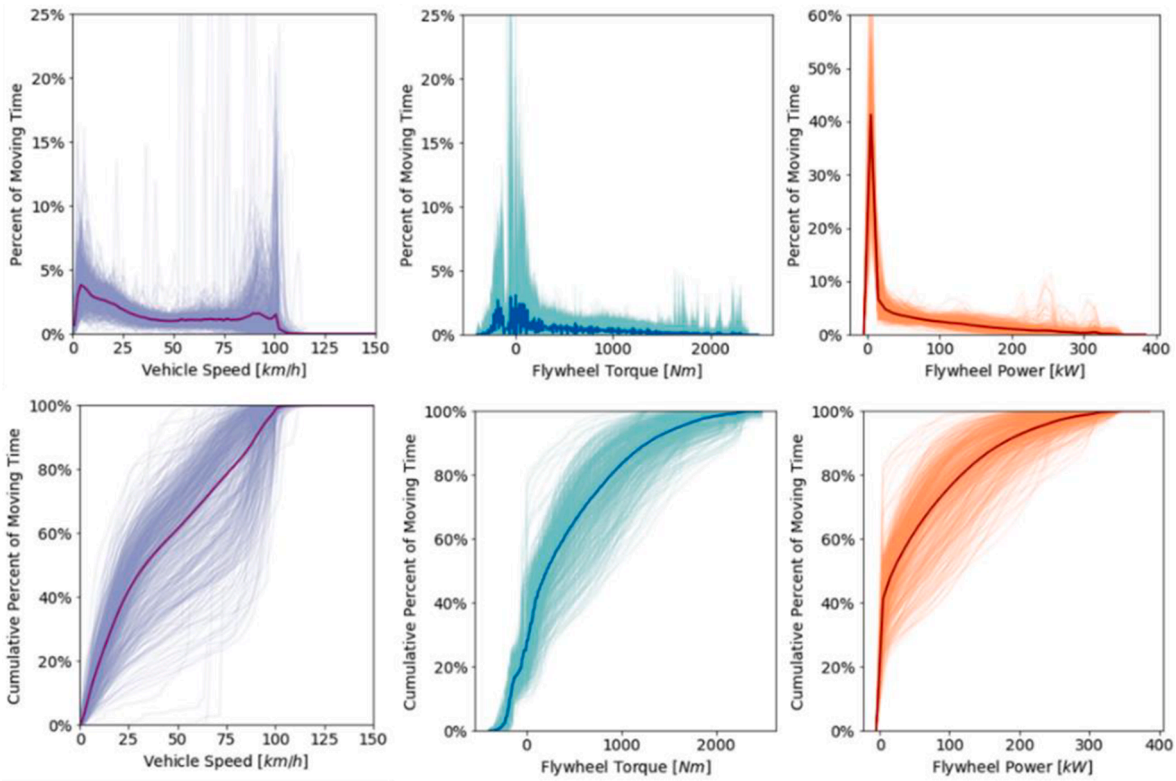

Fig. 4. Vehicle speed, engine torque, and power distribution based on moving time in drayage.

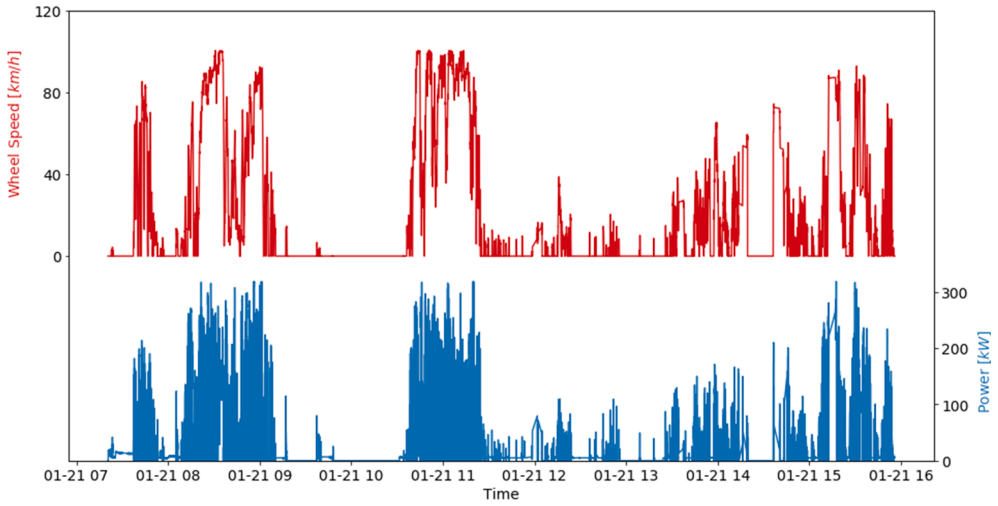

Fig. 5. Drayage daily trip with the most representativeness.

$$v_{aero}^2 = \frac{\sum_{j=1}^{N-1} \overline{v_{j,j+1}^3} \cdot \Delta t_{j,j+1}}{D} \tag{2}$$

where $v_{j,\,j+1}$ shows the average speed within the time period $\Delta t_{j,\,j+1}$.

Finally, the kinetic intensity is the ratio of characteristic acceleration to aerodynamic velocity, which provides a ratio of energy used to accelerate vs. energy used to overcome drag. All above three metrics have a strong correlation with fuel economy, energy consumption, and the ability to recapture energy, such as in hybridized or electrified powertrains.

The power-weighted work is a cycle metric indicating the power profile during a trip. We will revisit it in the next section (check Eq. (6) in Section 4.1.2.3).

Regression targets are derived for each daily trip using these metrics, followed by DTR, which is implemented to determine the

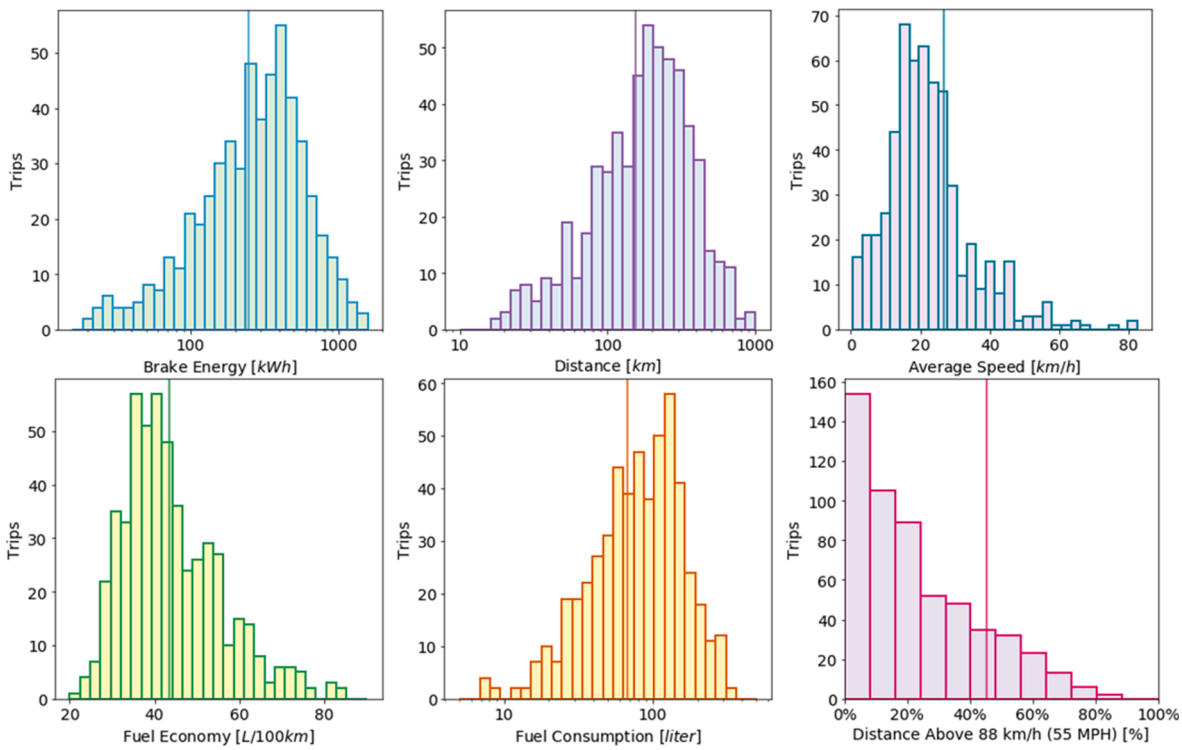

Fig. 6. Metrics of the most representativeness trip (vertical line) in the corresponding distributions from drayage.

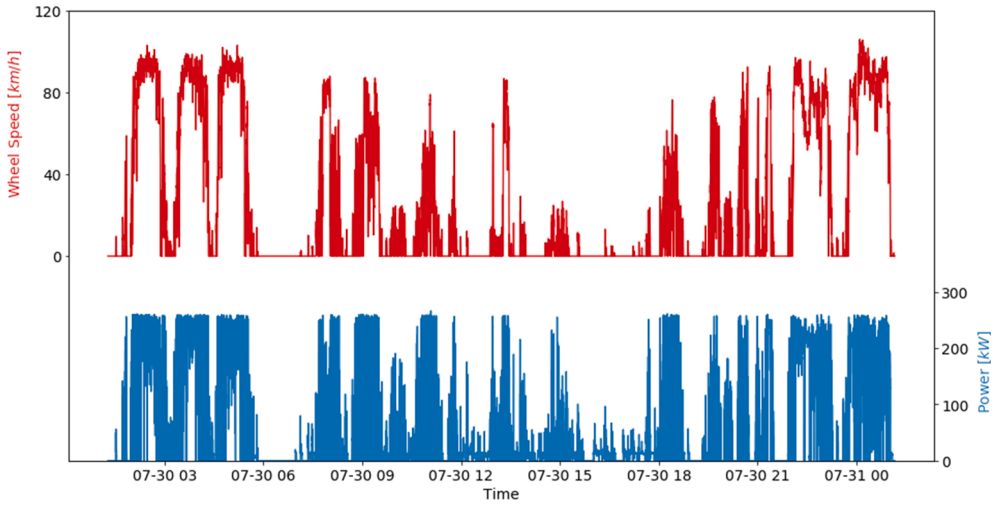

Fig. 7. Drayage daily trip with the maximal energy consumption.

importance of each metric to the target. This is shown as the weight value in Table 2. One beauty of applying the DTR is that the data itself will determine and explain which metrics are more important for representative cycle development, and those metrics can change based on vocation or vehicle population. If the speed and acceleration play significant role, they will be assigned a larger weighted number to account their impacts. Or if other metrics are relatively more important to the regression target, larger weighed number will be assigned to them. In this study, fuel economy dominates in significance within the power parameter set, as expected. In the vehicle parameter set, all metrics contribute to characterize the driving behavior, but percent time in idle is the most important. It should be noted that the weight values of different metrics are very sensitive to the vehicle vocation. Table 2 corresponds only to results obtained for drayage, and the rest of Section 3 also presents analysis referring only to drayage. The DTR results of the other four vocations are shown in Appendix A. It worth noting that from Appendix A, it is clear that metrics have different weighted numbers for each vocation. In other words, because driving behavior is completely different per vocation, each metric considered in this study has a different extent of influence on the regression target—specific energy consumption.

One of the challenges in developing the DTR model is to avoid "overfit." Overfit represents a situation where the DTR leans too finely upon the training data and learns from the noise instead of data with value. To ensure proper fitting of a DTR model, a small training set of data (including 70% of the total candidate pool) is used in this study to fit the model, and the remaining data are used to test the model by calculating the MSE. Furthermore, to avoid any influence of potentially abnormal data, this separation method was proceeded randomly 25 times. The evolution of the MSE along the tree depth is shown in Fig. 3. Each solid line represents the average MSE of each parameter set, whereas the colored shading represents the related standard deviation of the MSE. A tree depth of 7 was chosen for this model, which provided the lowest MSE for power metrics. Although this was not the lowest MSE for the route and vehicle metrics, the small increase in error provided weightings for all the metrics.

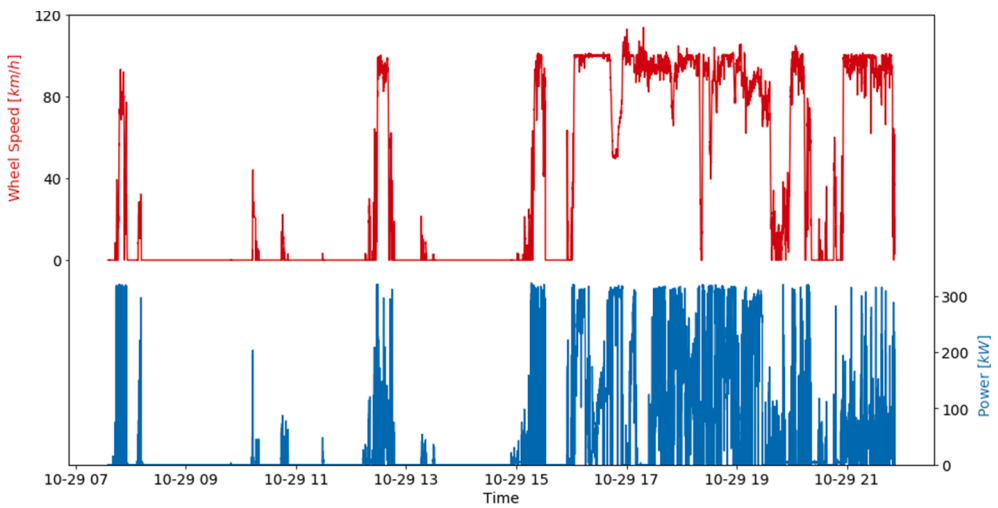

Fig. 8. Drayage daily trip with the maximal power-weighted work.

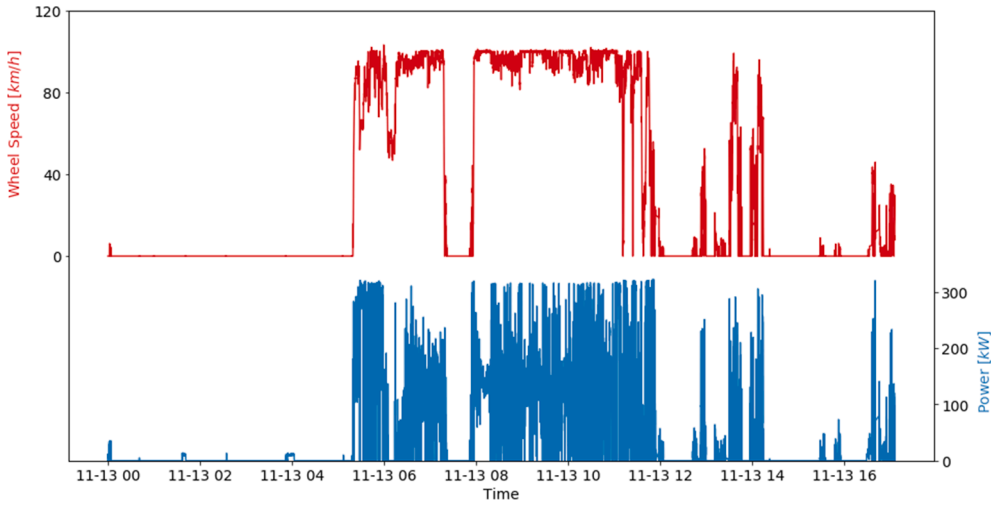

Fig. 9. Drayage daily trip with the maximal time duration at high speed.

After weighting the metrics with the DTR analysis, the z-score was calculated for each metric using Equation (3) (using brake-specific fuel consumption [BSFC] as an example):

$$Z_{BSFC\_i} = \frac{X_{trip(i)} - meanX_{alltrips}}{Std.Dev.X_{alltrips}} \tag{3}$$

The output of Eq. (3), the z-score of the BSFC metric in daily trip *i*, was weighted using the corresponding weight value in Table 2, and the weighted z-score was derived using Eq. (4):

$$\widetilde{Z}_{BSFC\_i} = w_{BSFC} \cdot Z_{BSFC\_i} \tag{4}$$

It is worth noting that for different vocations, the weight value is distinct even for the same metric. The other weighting values are listed in Appendix A. After developing the weighted z-score for each metric, the resulting scores of the daily trip *i* were combined using Eq. (5), which provides a single ranking metric for each daily trip:

$$Z_i = \sum \sqrt{\widetilde{Z}^2_{BSFC\_i} + \widetilde{Z}^2_{MPG\_i} + \cdots \widetilde{Z}^2_{speed\_i}} \tag{5}$$

Finally, the daily trip with the lowest z-score was selected as the representative route.

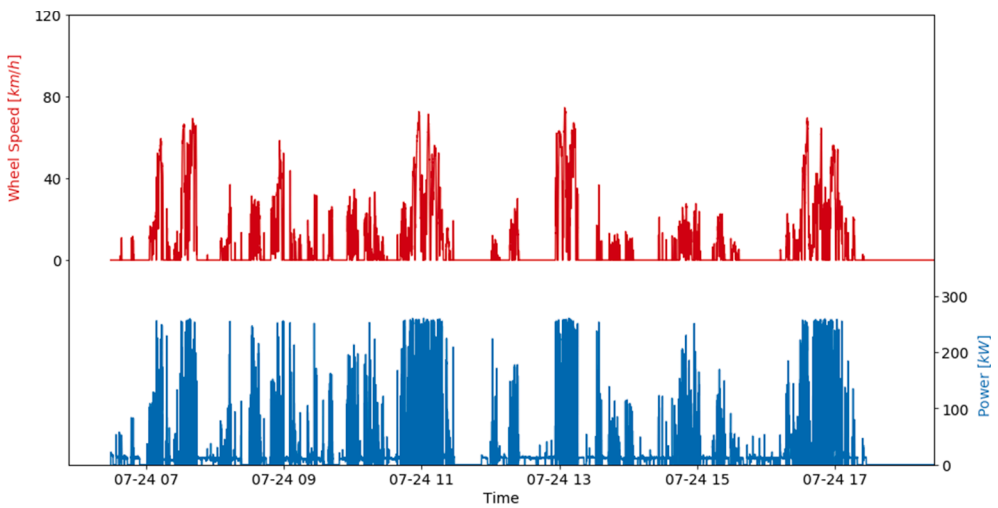

Fig. 10. Drayage daily trip with the minimal fuel economy.

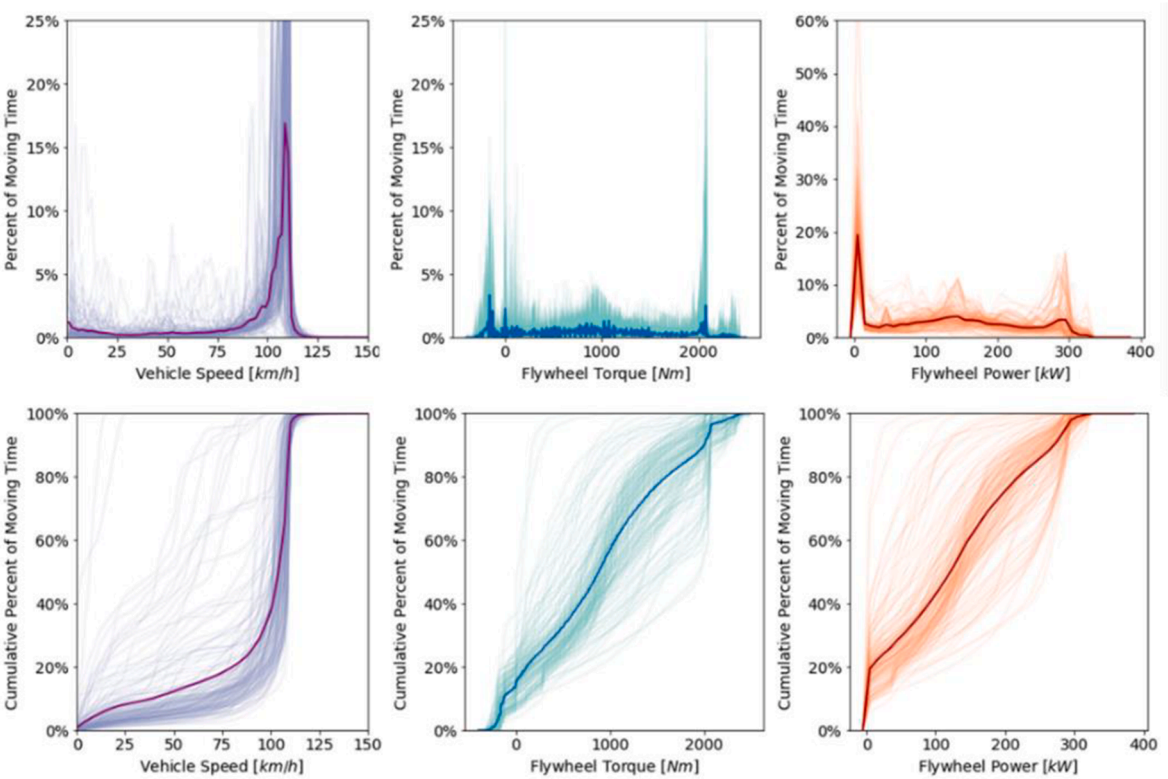

Fig. 11. Vehicle speed, engine torque, and engine power distribution based on moving time in long haul.

4. Results and discussion

Results of each vocation will be illustrated and discussed in this section. For each vocation, high-level statistical information is described first. This statistical information includes vehicle speed distribution, engine output torque distribution, and engine output power distribution based on vehicle moving time in each vehicle day, as well as the related cumulative distributions. Additionally, the average distributions of vehicle speed, engine torque, and power are shown on top of the entire spectrum, which reflects the corresponding distribution in general.

Following the duty cycle analysis are five representative driving cycles in each vocation—the cycle that is most representative from the DTR approach, the cycle with the maximal energy consumption, the cycle with the maximal power-weighted work, the cycle with

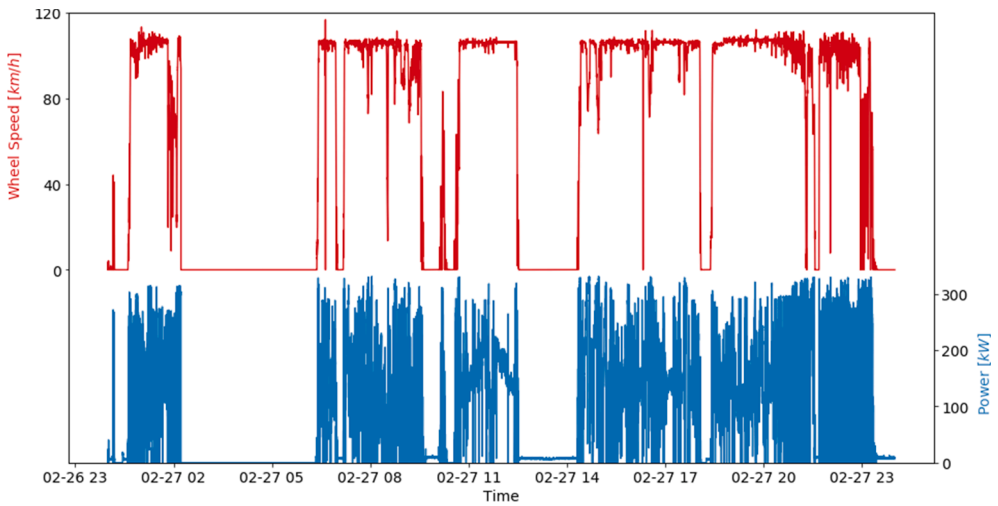

Fig. 12. Long-haul daily trip with the most representativeness.

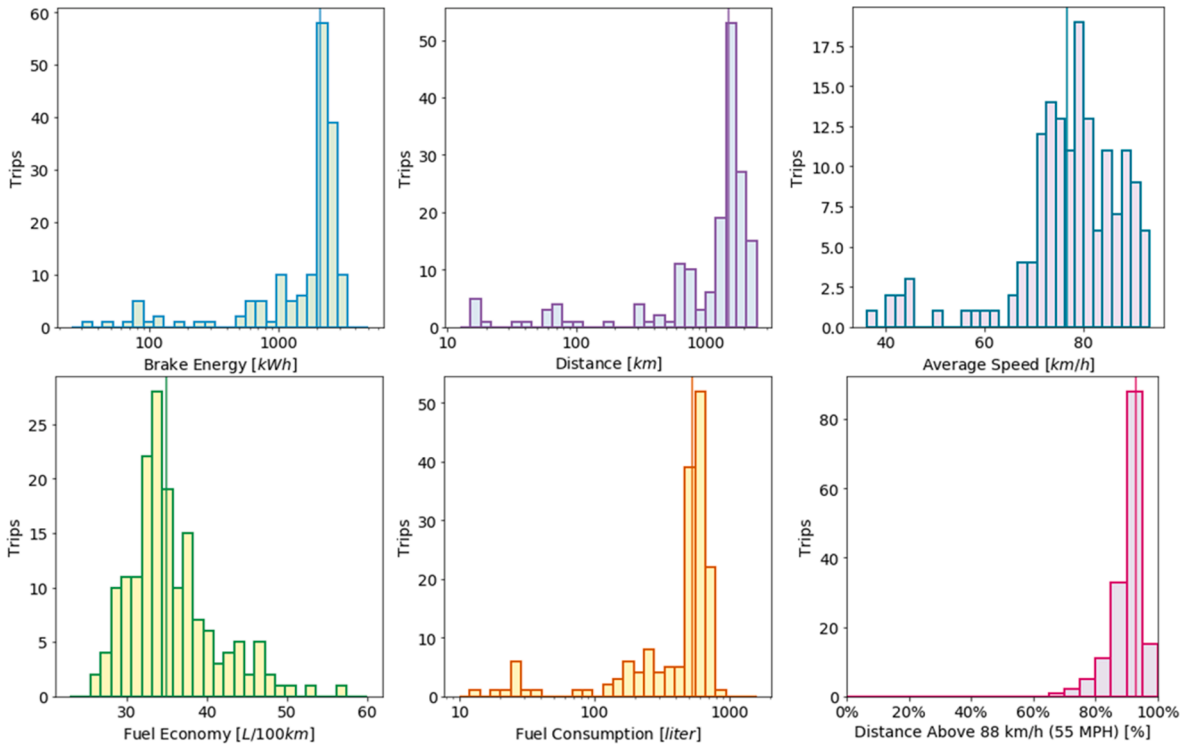

Fig. 13. Metrics of the most representativeness trip (vertical line) in the corresponding distributions from long-haul.

the maximal percentage of high speed (over 88 km/h), and the cycle with the minimal fuel economy—each illustrated with the vehicle speed and engine power profiles. The related detailed drive cycle data will be provided for free on NREL's DriveCAT website: https://www.nrel.gov/transportation/drive-cycle-tool/. For the most representative cycle, six daily trip metrics—energy output, fuel economy, daily trip distance, fuel consumption, average speed, and fraction of driving distance over 88 km/h (55 mph)—are highlighted by indicating their location in the corresponding metric distributions. Tables are also appended to describe the characteristics of the other four cycles by listing several corresponding metrics.

4.1. Drayage

Drayage trucks transport goods over a short distance in the shipping and/or logistics industries. It is often a part of a longer overall move and widely operated in seaports, inland ports, or intermodal terminals with both the trip origin and destination in the same urban area. Drayage trucks are usually weight Class 7 to 8 heavy-duty trucks and consist of a tractor and shipping container trailer (Prohaska et al., 2016).

4.1.1. Vehicle speed and engine operation distribution

Fig. 4 shows the statistical information based on the detailed on-road data collected from drayage trucks. For each subfigure, the entire distribution of data is depicted as a group of transparent curves, with each curve showing a daily trip distribution. By showing all the curves together, it is easy to identify the highest frequency of operating vehicle speeds, engine torques, and powers from the entire spectrum. In addition, the related dark curve in each subfigure indicates the average distribution derived from the related total daily distributions. The top row of graphs shows the distribution of data as a percentage for a given point on the x-axis, whereas the bottom row shows cumulative distributions.

No significant spikes exist in the average vehicle speed distribution for drayage, although high percentages of low speed and speed

Table 3
Metrics related to other cycles for long-haul trucks.

Driving Cycles	Distance (km)	Energy Cost (kWh)	Fuel Economy (l/100 km)	Average Speed (km/h)
Max. total energy consumption	2,149.9	3,306.9	37.6	90.8
Max. percentage of high speed	2,022.8	2,271.1	27.6	92.3
Max. power-weighted work	324.7	749.9	58.8	72.4
Min. fuel economy [a]	324.7	749.9	58.8	72.4

[a] The driving cycle with maximal power-weighted work is the same cycle as the minimal fuel economy in the long-haul vocation.

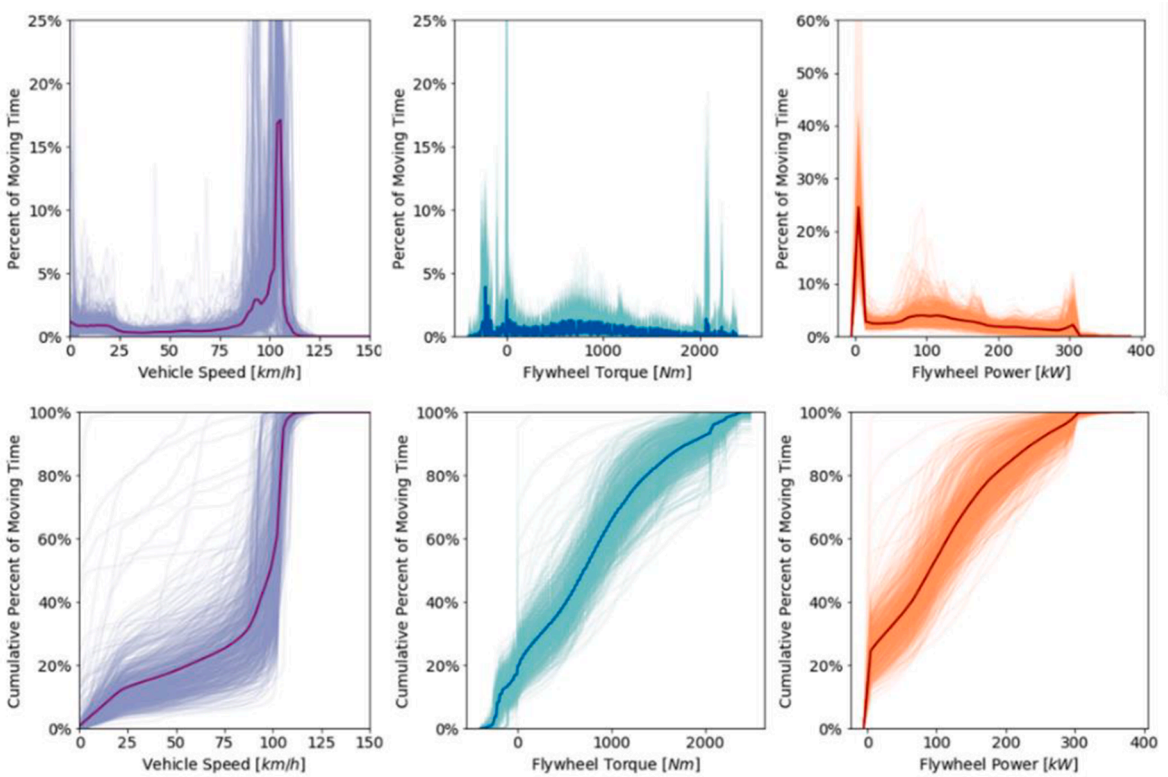

Fig. 14. Vehicle speed, engine torque, and engine power distributions based on moving time in regional-haul trucks.

around 96 km/h (60 mph) appear in the full data spectrum. Also, from the cumulative distribution, the vehicle speed is less than 64 km/h (40 mph) for 60% of the time and higher than 96 km/h (60 mph) for approximately 20% of the time. The engine torque and power distributions also show that the low-load situation is dominant in normal drayage operation; 70% of moving time exhibits power less than 100 kW, and for 80% of time, the torque is less than 1,000 Nm. Note that there are negative torques in the distribution, which reflects the on-road engine brake events.

4.1.2. Specific driving cycles

4.1.2.1. Most representative. Fig. 5 shows the vehicle speed and engine power vs. time for the daily trip with the most representative

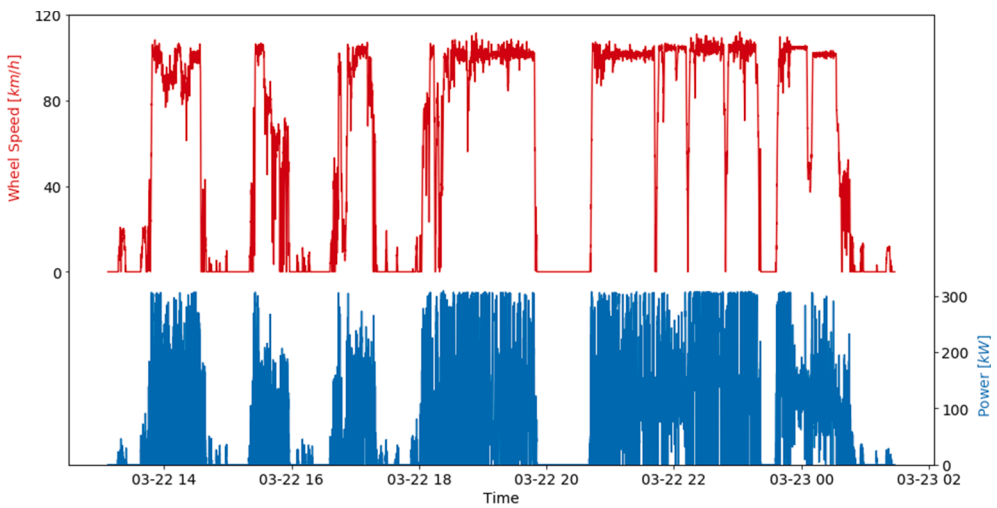

Fig. 15. Regional-haul daily trip with the most representativeness.

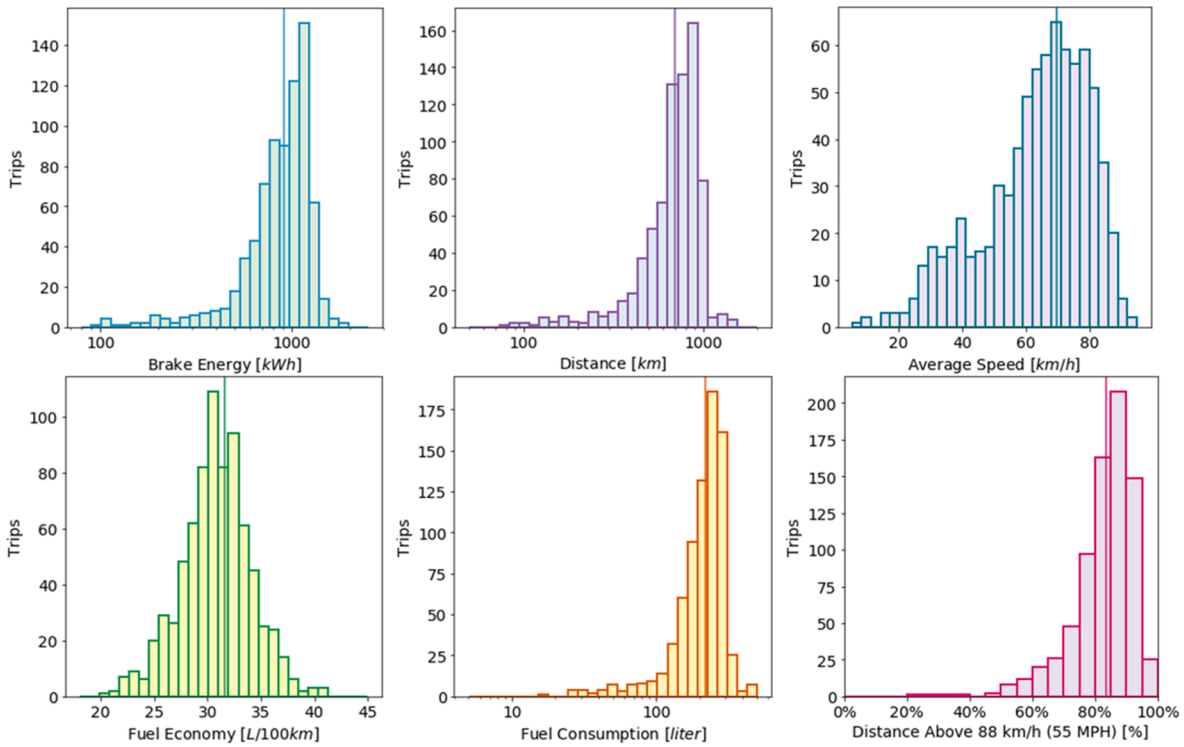

Fig. 16. Metrics of the most representativeness trip (vertical line) in the corresponding distributions from reginal-haul.

operation based on the DTR method for the drayage vocation. The format of the x-axis shows the date (January 21) and the hour of the day (0700 to 1600). The driving cycle starts at 7 a.m. and ends around 4p.m., which is the typical working day schedule. The vehicle experienced multiple high-speed driving (over 96 km/h, or 60 mph) sections, frequent stop-and-go sections, and even some long-duration idling periods. Such driving behaviors are normal in the drayage vocation, where vehicles wait in long queues, load, and unload goods in depot stations or at the port, and sometimes transfer the payload to other destinations with a long distance between origin and destination. Referring to the driving cycle shown in Fig. 5, the trip distance was around 156.3 km (97.1 miles) and produced over 245 kWh of flywheel energy. The fuel economy was approximately 43.6 L per 100 km (5.4 miles per gallon [mpg]), which is relatively low, mainly due to the frequent low-load operation and long periods of idling. Such driving characteristics can also be reflected by the average speed of the vehicle, which is only 26.8 km/h (16.7 mph).

To demonstrate the representativeness of the selected driving cycle, six metric distributions are shown in Fig. 6, with a vertical line to identify where this cycle falls within each distribution. As expected, the vertical lines usually occur near the mean of the distributions; however, those values with lower weighting fall further from the mean. As a side note, these distributions reflect specific statistical information relevant to the drayage vocation. For example, the fuel economy of the drayage truck ranged from 20 to 80 L per 100 km, and the daily brake energy or energy produced from the engine at the flywheel can be over 1,000 kWh for drayage trucks. It is worth noting that all of these metrics are recorded or derived based on the on-road engine CAN bus data, with the engine brake-specific energy (shorten as brake energy in Fig. 6) derived from the engine torque and speed signals and the fuel economy derived from the instantaneous fuel rate signals.

4.1.2.2. Maximal energy consumption. Fig. 7 shows the daily trip with the maximal daily energy consumption from drayage. This daily trip includes travel from 2 a.m. to midnight, producing 1,534.3 kWh of brake energy. Considering the fluctuation in the speed profile, the vehicle accelerates and deaccelerates frequently, thus producing relatively lower fuel economy (49.0 L per 100 km, or 4.8 mpg). This is also why the trip uses so much fuel, even though the distance is only 605.6 km (376.3 miles). The longest daily trip distance of

Table 4
Metrics related to other cycles for regional-haul trucks.

Driving Cycles	Distance (km)	Energy Cost (kWh)	Fuel Economy (l/100 km)	Average Speed (km/h)
Max. total energy consumption	1,421.9	1,801.5	38.8	68.3
Max. percentage of high speed	1,259.2	1,466.6	27.6	89.9
Max. power-weighted work	924.9	1,350.6	33.7	53.6
Min. fuel economy	564.9	851.3	41.0	56.9

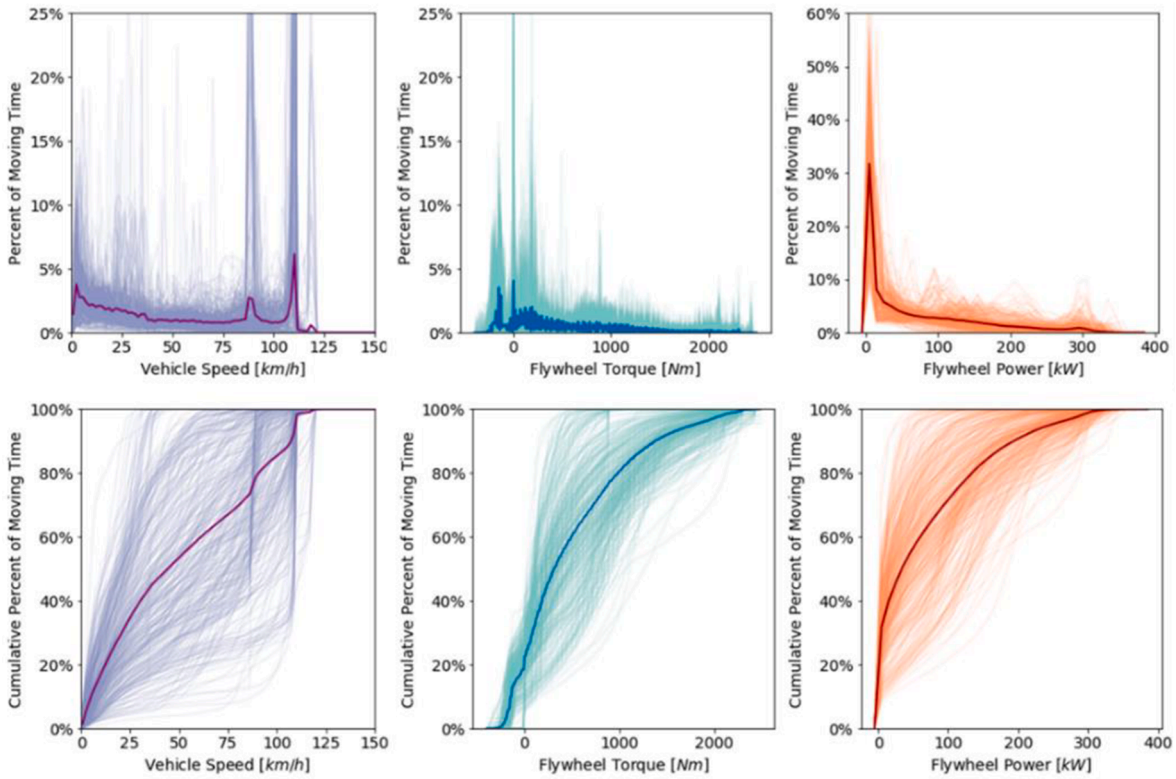

Fig. 17. Vehicle speed, engine torque, and engine power distribution based on moving time in local delivery.

the recorded drayage data is around 997.8 km (620.0 miles).

4.1.2.3. Maximal power-weighted work. The power-weighted work, W_{power}, is calculated as:

$$W_{power} = \sum_t \frac{P_t^2}{(\sum_t P_t)} \cdot \Delta t \tag{6}$$

where P_t is the instantaneous engine output power and $\sum_t P_t$ is the sum of all the instantaneous engine output powers, and Δt is the sample time, which is 1 s in this study.

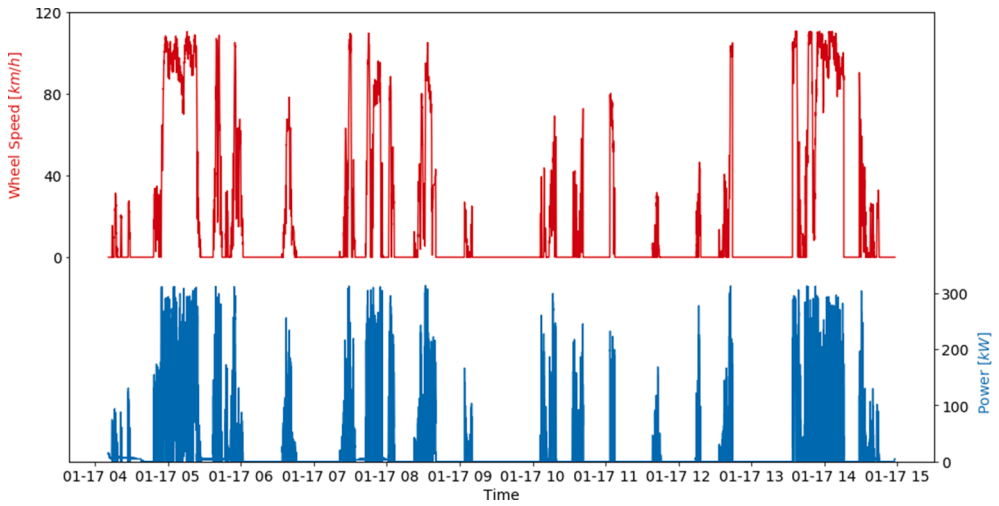

Fig. 18. Local delivery daily trip with the most representativeness.

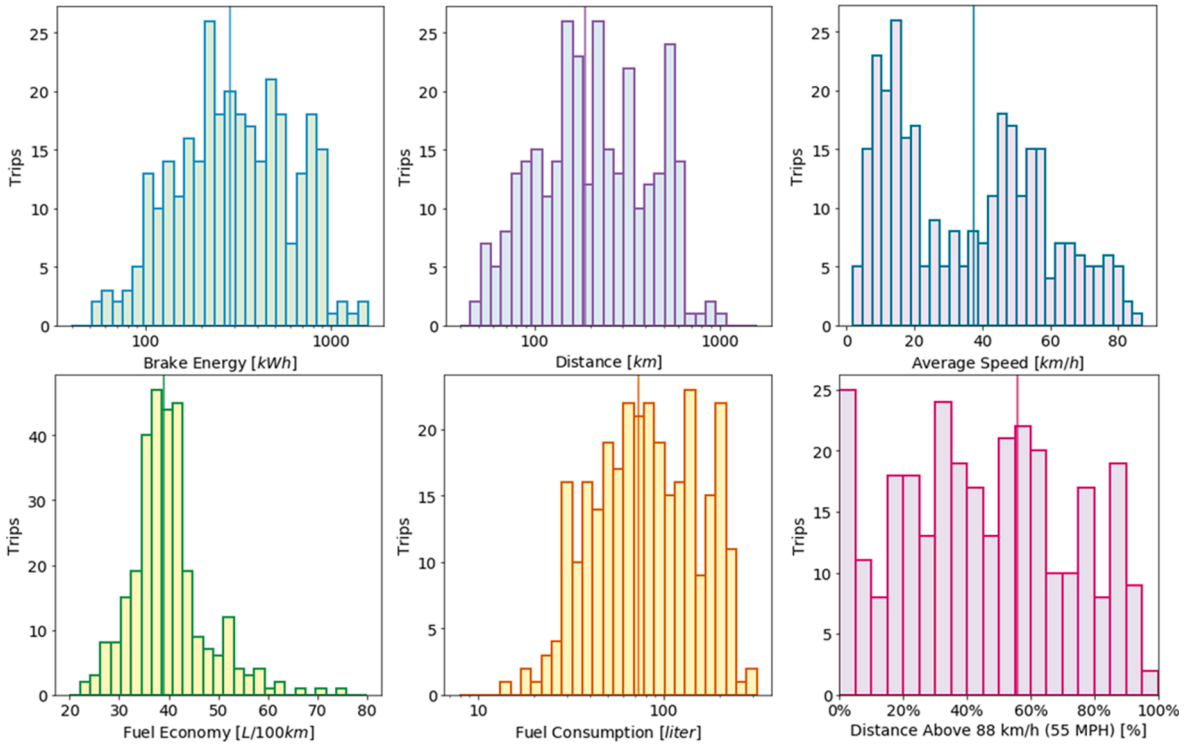

Fig. 19. Metrics of the most representativeness trip (vertical line) in the corresponding distributions from local delivery.

Usually, the daily trip with larger power-weighted work requires higher peak and sustained power demand from the power source (e.g., internal combustion engine or electrical motor). Therefore, it is reasonable to investigate this trip and analyze whether an alternative powertrain can satisfy this extreme power demand. It is worth noting that in the internal combustion engine case, the peak power is a mechanical measure at the engine flywheel, whereas the associated power demand on an electric vehicle would need to be converted to an electrical power considering electrical transfer and conversion efficiency.

Fig. 8 shows the details of the daily trip with the maximal power-weighted work. In some cases, the vehicle needs to accelerate from stop to almost 96 km/h (60 mph) within a short time, which requires aggressive peak power. As a result, such a trip, which is only 506.6 km (314.8 miles), demands 225.0 kJ power-weighted work. Other properties of this daily trip include a flywheel energy production of 721.9 kWh, fuel economy of 36.8 L per 100 km (6.4 mpg), and average speed of 55.2 km/h (34.3 mph).

4.1.2.4. Maximal time duration at high speed (over 88 km/h, or 55 mph). Fig. 9 shows the daily drayage trip with maximal high-speed fraction. In this daily trip, the vehicle mainly operates from 5 a.m. to 4p.m. In the early morning (from midnight to 4 a.m.), the vehicle also idles multiple times. Within the major operation duration, the vehicle drove above 88 km/h (55 mph) over 57% of the time, which is the largest fraction in the entire drayage data set. Consequently, the vehicle also possesses a higher fuel economy of 34.3 L per 100 km (6.9 mpg) and a faster average speed of 55.5 km/h (34.5 mph).

4.1.2.5. Minimal fuel economy. The final trip is the daily trip with the minimal fuel economy. As shown in Fig. 10, the derived trip operates from 6 a.m. to 5p.m. with extensive idle operation. The vehicle speed never passes 72 km/h (45 mph), indicating that the vehicle only operates at a depot or on local roads. As a result, the fuel economy associated with this daily trip is only 84.9 L per 100 km (2.77 mpg), and the average speed is 16.3 km/h (10.2 mph). Even though the trip distance is only 87.5 km (54.4 miles), the total flywheel energy production reaches 334.6 kWh, which is in the middle of the related distribution in Fig. 6.

Table 5
Metrics related to other cycles for local delivery trucks.

Driving Cycles	Distance (km)	Energy Cost (kWh)	Fuel Economy (l/100 km)	Average Speed (km/h)
Max. total energy consumption	1,058.1	1,504.1	35.7	56.9
Max. percentage of high speed	439.3	569.4	32.9	87.0
Max. power-weighted work	251.7	562.0	52.8	56.9
Min. fuel economy	78.7	235.4	75.4	5.2

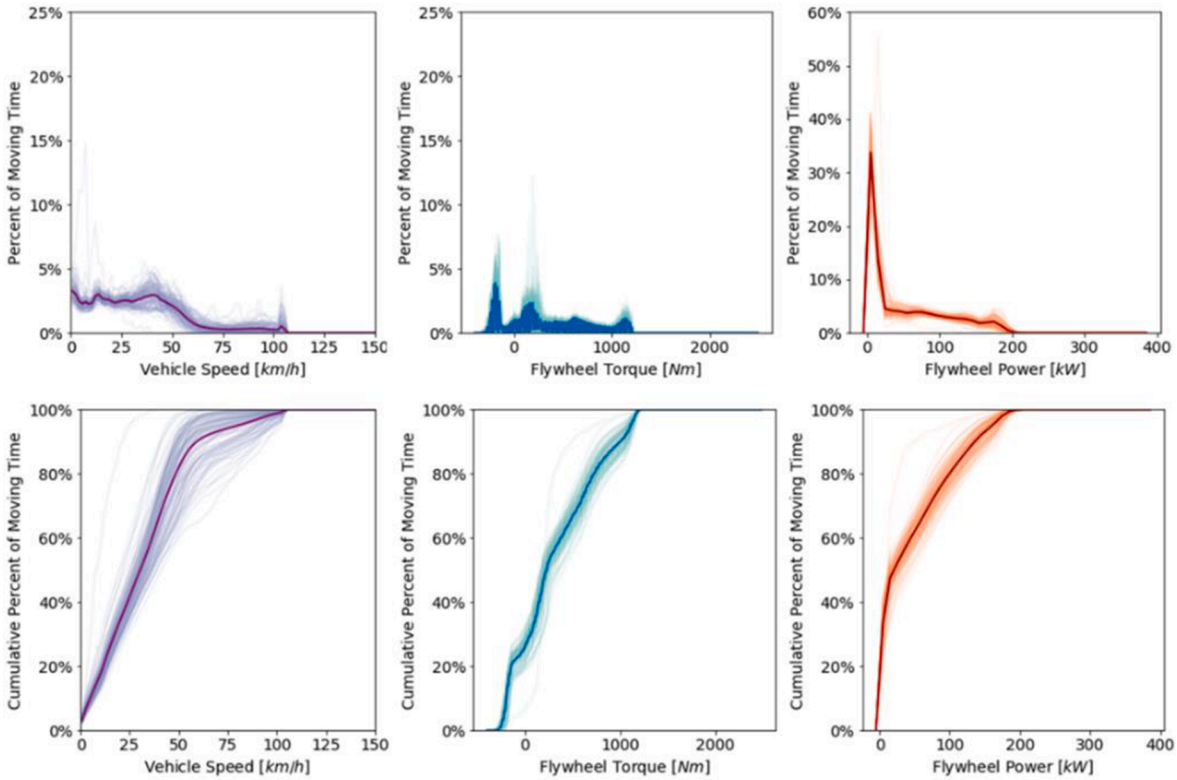

Fig. 20. Vehicle speed, engine torque, and engine power distribution based on moving time in transit bus.

4.2. *Long haul*

Long-haul trucks are typically weight Class 7 to 8 tractor-trailer combinations, used to transport various types of freight over long distances with sleeper cabs. These vehicles are usually driven on interstate highways with moderate road grades, and average driven mileage could be over 900 km (500 miles) per day. In this study, the trucks in the long-haul fleet are driven by a shifting team (two drivers take turns during operation). As a result, the daily driven distance and fuel consumption may be high, whereas speed and torque distribution still retain long-haul truck characterization. Daily driven distance reflects the extreme case for energy consumption, which is valuable to the design of the alternative zero-emission powertrain systems.

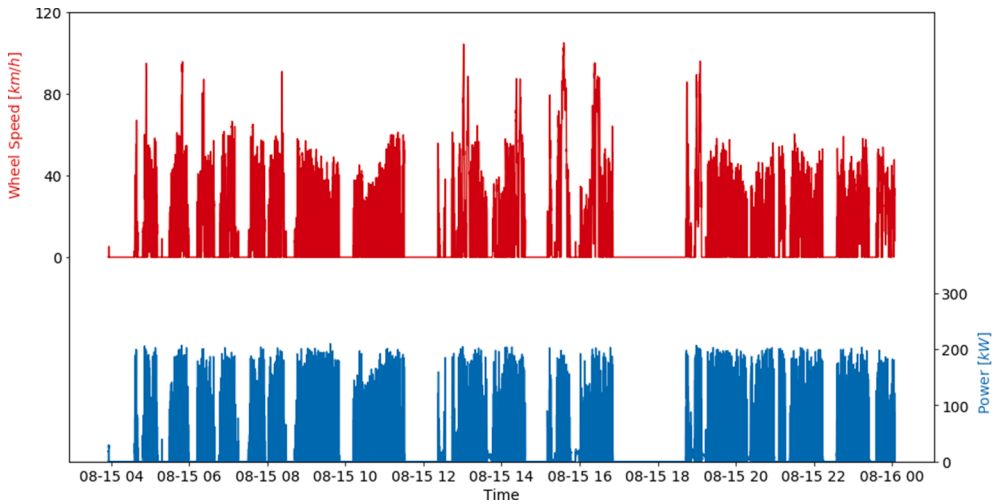

Fig. 21. Transit bus daily trip with the most representativeness.

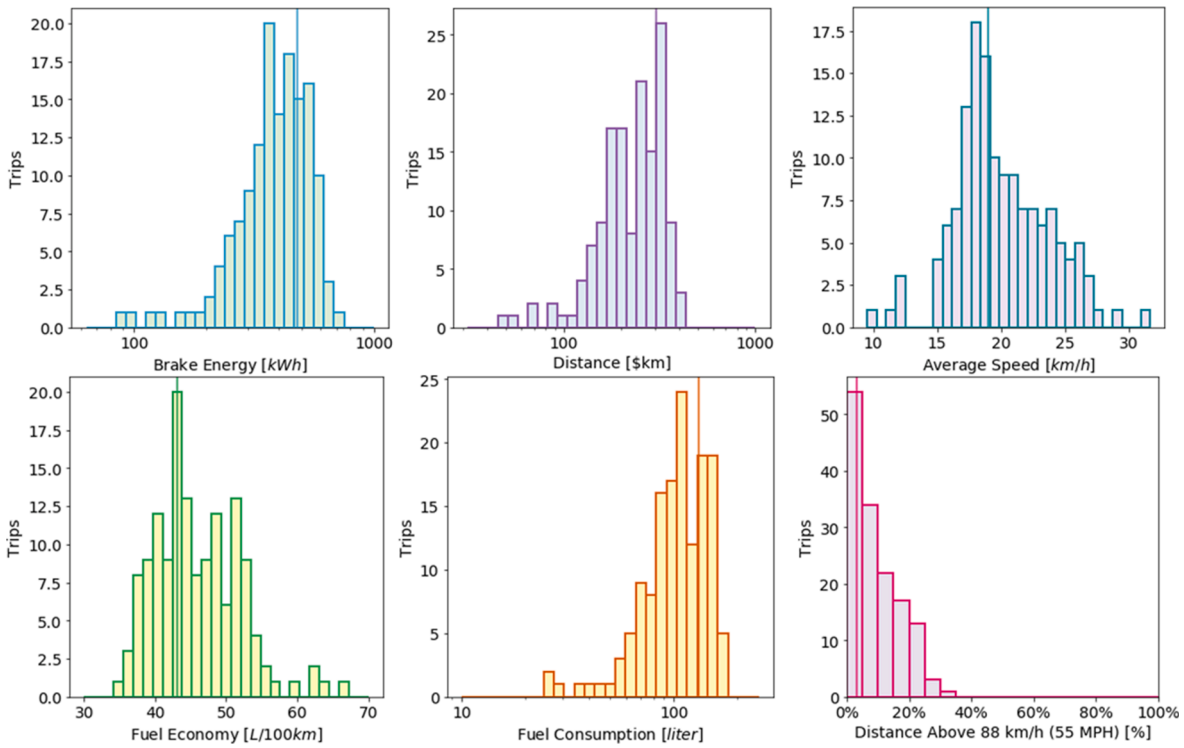

Fig. 22. Metrics of the most representativeness trip (vertical line) in the corresponding distributions from transit bus.

4.2.1. *Vehicle speed and engine operation distribution*

Fig. 11 depicts vehicle speed, engine torque, and power distributions for long-haul trucks. Considering that long-haul trucks mainly drive along interstate highways across the country, it is reasonable that a significant peak exists in vehicle speed distribution around 104 km/h (65 mph). In fact, more than 70% of total operation time occurred while the long-haul truck speed was over 96 km/h (60 mph), as shown in the cumulative distribution of vehicle speed. Although a typical engine for long-haul trucks is sized for 300-kW power and over 2,000-Nm torque, low-load conditions still represent a significant portion of the engine torque and power distribution in this vocation. This is exemplified by the wide, non-zero distribution of flywheel power less than 300 kW and a spike around the peak power. Besides the driving loads, the hoteling load in long-haul trucks can further contribute to the fraction of low-load conditions. As Fig. 11 shows, long-haul trucks only require minimal engine output torque (less than 300 Nm) and mild power (less than 10 kW) around 20% of the time.

4.2.2. *Most representative driving cycle*

Fig. 12 shows the most representative driving cycle based on the DTR method for long-haul trucks. The entire daily trip lasts almost 24 h, indicating that the truck is driven by a team with shift duty. In addition, this vehicle was parked between 2 a.m. and 6 a.m. for a rest and idled from noon to 1:30 p.m. for a break. Another apparent characteristic of this driving cycle is that the vehicle speed mainly sustains at 104 km/h (65 mph), with some small amplitude fluctuation (maybe caused by traffic along the interstate highway or variations in road grade). The derived driving cycle includes over 1,513 km (940 miles) with average speed 76.8 km/h (47.7 mph). The vehicle produced more than 2,123 kWh of flywheel energy with a fuel economy of 35.1 L per 100 km (6.7 mpg).

The metrics distributions in Fig. 13 offer more information related to the driving characteristics in long-haul trucks, with the representative route indicated by the vertical line in each distribution. For this specific fleet, the long-haul trucks drove around 1,609 km (1,000 miles) per day and produced over 1,200 kWh of flywheel energy from over 400 L of diesel. Due to such long daily trip distances, superior fuel economy is in high demanded for this vocation to mitigate emissions production and fuel consumption.

Table 6
Metrics related to other cycles for transit bus.

Driving Cycles	Distance (km)	Energy Cost (kWh)	Fuel Economy (l/100 km)	Average Speed (km/h)
Max. total energy consumption	340.8	687.1	52.2	18.3
Max. percentage of high speed	328.9	436.1	35.7	31.7
Max. power-weighted work[a]	328.9	436.1	35.7	31.7
Min. fuel economy	87.3	227.0	67.0	11.5

[a] The driving cycle with maximal power-weighted work is the same cycle as the maximal high-speed percentage in the transit bus vocation.

However, from Fig. 13, the related fuel economy distribution ranges from 25 to 55 L per 100 km, meaning there is a large potential for fuel economy improvement on some routes. Finally, the majority of the daily trip distance is driven at high speed (over 88 km/h, or 55 mph), and the average speed of long-haul trucks per day is around 80 km/h.

For the sake of conciseness, the other four driving cycles for long-haul, as well as the rest of the vocations, are included in Appendix B. Table 3 offers several metrics related to these four cycles to offer general information. It should be noted that the maximal power-weighted work cycle in the long-haul vocation is also the minimal fuel economy. From Appendix B, it is clear that unlike the other cycles in the long-haul vocation, the vehicle speed profile in this cycle fluctuates significantly. Such frequent accelerations and deaccelerations require aggressive power demand and reduce the fuel economy.

4.3. Regional haul

Like long-haul trucks, regional-haul trucks also refer to Class 8 semi-trucks (and may include some Class 7 trucks as well) that transfer goods moderate distances. As defined by the North American Council for Freight Efficiency, regional-haul trucks usually operate within a 480-km (300-mile) radius of a home base. This may include tractors that return to a home base every day or ones on routes for multiple days but within that 480-km (300-mile) radius (Mihelic and Roeth, 2019). As a result, they may still drive longer than 500 km per day.

4.3.1. Vehicle speed and engine operation distribution

As mentioned previously, regional-haul trucks usually operate in a similar way to long-haul trucks, except that the daily trip distances are shorter, and the vehicles are mainly driven within a state. These facts are reflected in Fig. 14, which depicts the high-level statistic characteristics of regional-haul truck operation. A clear spike also exists in the speed distribution around 104 km/h (65 mph) in regional haul, and the low-load conditions still dominate the entire distributions of engine torque and power.

4.3.2. Most representative driving cycle

The most representative cycle based on the DTR method for regional haul (Fig. 15) also reflects similarity to long-haul trucks to some extent. Most of the vehicle speed in regional haul is around 104 km/h (65 mph). However, unlike long haul, the regional-haul trucks parked more frequently during the daily trip, which is indicative of the short distances between multiple destinations. In addition, the regional-haul trucks exhibit less idle time during the day, whereas the long-haul trucks idle frequently for breaks.

The difference between the driving behaviors of regional- and long-haul trucks are more obvious from the metrics distributions in Fig. 16. As can be seen, the majority of daily trip distance of regional haul is less than 1,000 km (620 miles) and the average speed is less than 72.4 km/h (45 mph); both are less than the counterparts from long haul (around 1,400 km and 83.7 km/h, respectively). Intuitively, the corresponding fuel and energy consumption from regional haul are also less. The shape of the fuel economy distribution from reginal haul is almost identical for long haul, but with relatively larger values in the range of 20–40 l/100 km. The vertical lines again show the representativeness of the derived cycle.

Table 4 shows the corresponding statistics of the other four cycles for regional haul. The detailed information related to each of them can be found in Appendix B.

4.4. Local delivery

Local delivery trucks refer to trucks that transfer goods such as beverage, food, and linen from a distribution facility to grocery stores, supermarkets, or other businesses centers. As a result, the trucks usually drive along both urban local roads and interstate highways. Consequently, the driving behavior of local delivery trucks can vary a lot in practice.

4.4.1. Vehicle speed and engine operation distribution

As shown in Fig. 17, the observed vehicle speed distribution possesses two spikes, located around 64 km/h (40 mph) and 104 km/h (65 mph). In fact, the vehicle's speed is less than 64 km/h (40 mph) around 70% of the time and higher than 96 km/h (60 mph) 20% of the time. The engine torque and power distributions are similar to regional haul and long haul but are still dominated by low-load conditions, mainly from the low-speed driving within the urban area.

4.4.2. Most representative driving cycle

The most representative driving cycle based on the DTR method for local delivery is shown in Fig. 18. The vehicle speed shows that the truck experienced interstate highway (indicated by high speed), urban routes (indicated by low speed), and multiple stop-and-go situations. Further, the vehicle speed profile consists of multiple sections separated by several soak or engine-off periods that last more than 20 min, where the vehicle loads or unloads the cargo. This type of cycle clearly reflects operations where the trucks deliver goods to several destinations within a typical daily duty.

The metric distributions are far more scattered than the other vocations, especially for the distributions of average speed and distance driven at high speed. From Fig. 19, these two distributions possess visible fractions for all the bins with no singular peak, whereas energy consumption, fuel consumption, and trip distance are normal distributions with peaks located around 300 kWh, 100 l, and 160 km, respectively. The fuel economy is normally distributed as well, with a peak around 40 l/100 km, lower than other vocations. Table 5 shows the corresponding statistics of other four cycles for local delivery.

4.5. Transit bus

Transit bus typically operates in metropolitan areas with shorter distance than the other studied vocations. Further, speeds typical in metropolitan areas are usually slower, and transit buses thus have lower power demands.

4.5.1. Vehicle speed and engine operation distribution

As shown in Fig. 20, both the speed and torque distributions of transit buses are much lower compared to the trucks in the other vocations. Specifically, the slower vehicle speeds (less than 64 km/h) cover more than 90% of moving time from the entire data set. Nonetheless, a few vehicles still reach high speeds (around 96 km/h). Such a situation may be caused by the fact that the bus needs to transition from one city to a nearby one. The engine torque and power distributions are distinct compared to the truck applications due to lower peak torque and power. More than 70% of moving time in transit buses requires output power less than 100 kW, and more than 90% of moving time requires engine torque less than 1,000 Nm.

4.5.2. Most representative driving cycle

The most representative cycle based on the DTR method for transit buses is shown in Fig. 21. This bus operates from 4 a.m. to almost midnight. Apparent route trips are separated with clear soak periods, usually lasting 20 min or longer. Within each route, the bus has frequent stop-and-go operation to pick up and discharge passengers. Longer soak periods around noon and late afternoon may reflect times when drivers take lunch and dinner breaks or when a driver changes.

The distributions of energy consumption, trip distance, and fuel consumption are normal distributions for transit bus, as shown in Fig. 22. The daily trip distance can be longer than 300 km, which is caused by almost 20 h of operation during a day. Due to the frequent stop-and-go travel, the average speed of the transit bus is much slower compared to the other vocations, with a peak located around 17.7 km/h (11 mph). Consequently, the fuel economy is not as high as the other vocations and is in the range of 35–70 l/100 km.

Table 6 shows the corresponding statistics of the other four cycles for transit bus. It should be noted that the cycle with maximum percentage of high speed possesses a highway section in each route. Additionally, the cycle with the minimal fuel economy idles during the period between each route, contributing to the low fuel economy value. Details can be found in Appendix B.

5. Conclusions

In this paper, we characterized the driving behaviors of five HD vocations—drayage, long haul, regional haul, local delivery, and transit bus—through Fleet DNA, an on-road commercial vehicle database. Both extreme driving behavior and representative driving behavior were determined in each vocation. The former behavior is explained by four different driving cycles with the maximal energy consumption, maximal power-weighted work, maximal fraction of high speed, and minimal fuel economy. Representative driving cycle in each vocation was derived through a novel approach using DTR. Unlike other methods, which only take speed and acceleration information into consideration, the proposed approach includes additional metrics such as engine power and fuel consumption and assigned each metric a weighted number to indicate the corresponding influence on the objective of the representativeness. The results of DTR clearly shows that due to the distinct driving behavior in each vocation, each metric affects the related fuel economy features differently. In this way, the representative cycle determined by such a weighted mean z-score was more accurate.

In the future, the detail drive cycle data will be uploaded on NREL's DriveCAT website: https://www.nrel.gov/transportation/drive-cycle-tool/. Beyond, additional metrics such as road grade, transmission gear ratio, and payload can be added into this approach to further enhance the representativeness. Additionally, if the data are available, the driving behavior of HD vocations in other regions like Europe and Asia can also be characterized. Furthermore, the derived representative and extreme driving cycles for each vocation can be applied to the system design and optimal control development for advanced electrical powertrains, as they indicate the statistical averages and outliers of key vocations.

Acknowledgments

This work was authored in part by the National Renewable Energy Laboratory, operated by Alliance for Sustainable Energy, LLC, for the U.S. Department of Energy (DOE) under Contract No. DE-AC36-08GO28308. Funding provided by Toyota Motor North America under a Cooperative Research and Development Agreement. The views expressed in the article do not necessarily represent the views of the DOE or the U.S. Government. The U.S. Government retains and the publisher, by accepting the article for publication, acknowledges that the U.S. Government retains a nonexclusive, paid-up, irrevocable, worldwide license to publish or reproduce the published form of this work, or allow others to do so, for U.S. Government purposes.

Appendix A

Long Haul
Table A.1.

Table A.1
Daily trip metrics along with DTR output – long haul.

Power Parameters	**Weight**
Brake-specific fuel consumption	55.66%
Fuel economy	44.34%
Vehicle Parameters	**Weight**
Power-weighted work	92.49%
Percent time in idle	3.23%
Total work	3.10%
Fuel consumed	1.18%
Route Parameters	**Weight**
Aerodynamic velocity	51.00%
Percent zero speed	15.22%
Stops per mile	9.68%
Percent of distance greater than 88 km/h (55 mph)	5.36%
Percent of distance less than 8 km/h (5 mph)	4.51%
Standard deviation driving speed	4.11%
Average speed	2.51%
Percent of distance at 8–24 km/h (5–15 mph)	2.50%
Max. speed	2.07%
Characteristic acceleration	1.35%
Trip distance	1.30%
Kinetic intensity	0.32%
Average driving speed	0.07%

Regional Haul
Table A.2.

Table A.2
Daily trip metrics along with DTR output – regional haul.

Power Parameters	**Weight**
Fuel economy	78.90%
Brake-specific fuel consumption	21.10%
Vehicle Parameters	**Weight**
Power-weighted work	33.86%
Percent time in idle	30.74%
Fuel consumed	23.68%
Total work	11.72%
Route Parameters	**Weight**
Characteristic acceleration	31.81%
Kinetic intensity	11.50%
Aerodynamic velocity	9.55%
Average speed	8.41%
Percent of distance greater than 88 km/h (55 mph)	8.05%
Trip distance	7.04%
Max. speed	5.42%
Percent of distance 8–24 km/h (5–15 mph)	3.74%
Percent zero speed	3.70%
Stops per mile	3.41%
Average driving speed	2.91%
Percent of distance less than 8 km/h (5 mph)	2.35%
Standard deviation driving speed	2.09%

Local Delivery
Table A.3.

Table A.3
Daily trip metrics along with DTR output – local delivery.

Power Parameters	**Weight**
Fuel economy	75.29%
Brake-specific fuel consumption	24.71%
Vehicle Parameters	**Weight**
Percent time in idle	42.52%
Fuel consumed	20.22%
Power-weighted work	19.94%
Total work	17.32%
Route Parameters	**Weight**
Trip distance	17.81%
Percent zero speed	16.34%
Aerodynamic velocity	14.62%
Characteristic acceleration	12.30%
Max. speed	10.27%
Stops per mile	7.03%
Kinetic intensity	5.39%
Average driving speed	3.79%
Percent of distance 8–24 km/h (5–15 mph)	3.77%
Percent of distance less than 8 km/h (5 mph)	3.52%
Percent of distance greater than 88 km/h (55 mph)	2.26%
Standard deviation driving speed	2.05%
Average speed	0.84%

Transit Bus
Table A.4.

Table A.4
Daily trip metrics along with DTR output – transit bus.

Power Parameters	**Weight**
Fuel economy	99.99%
Brake-specific fuel consumption	0.01%
Vehicle Parameters	**Weight**
Power-weighted work	99.41%
Percent time in idle	0.54%
Total work	0.03%
Fuel consumed	0.01%
Route Parameters	**Weight**
Kinetic intensity	99.09%
Stops per mile	0.79%
Characteristic acceleration	0.05%
Percent zero speed	0.03%
Trip distance	0.02%
Percent of distance less than 8 km/h (5 mph)	0.01%
Max. speed	0.01%
Aerodynamic velocity	0.00%
Standard deviation driving speed	0.00%
Percent of distance greater than 88 km/h (55 mph)	0.00%
Percent of distance 8–24 km/h (5–15 mph)	0.00%
Average speed	0.00%
Average driving speed	0.00%

Appendix B

Long Haul

- Maximal energy consumption

  Fig. B.1.

- Maximal power-weighted work

  Fig. B.2.

- Maximal time duration at high speed

  Fig. B..3.

- Minimal fuel economy

  Same as maximal power-weighted cycle in long-haul vocation

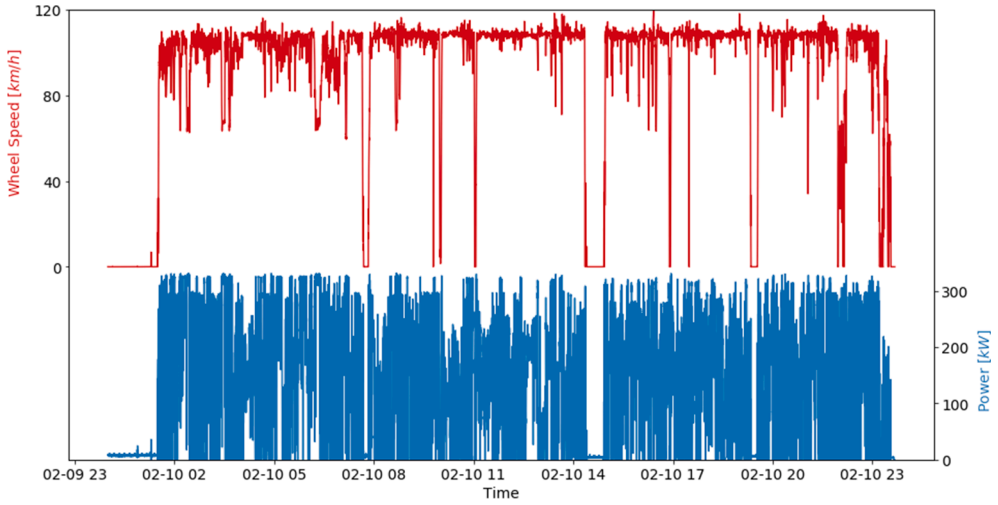

Fig. B.1. Long-haul daily trip with the maximal energy consumption.

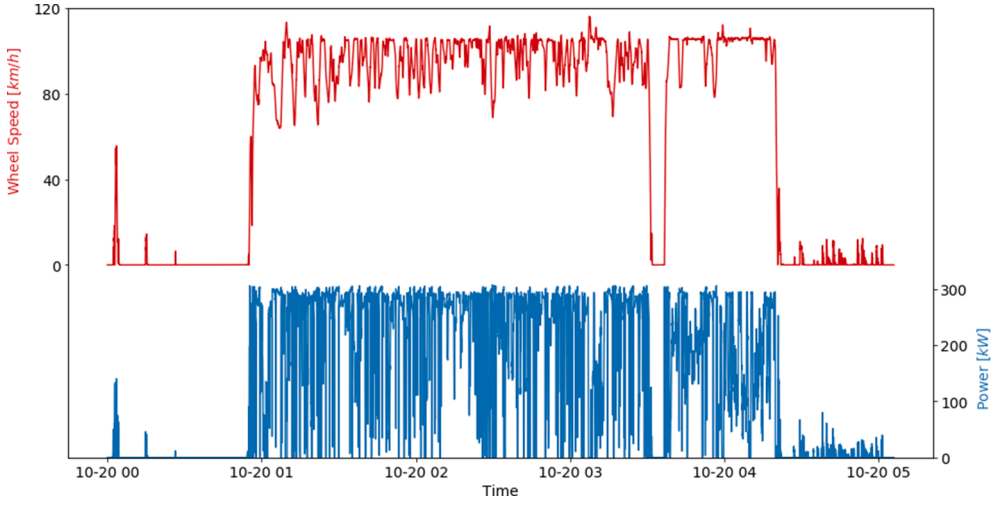

Fig. B.2. Long-haul daily trip with the maximal power-weighted work.

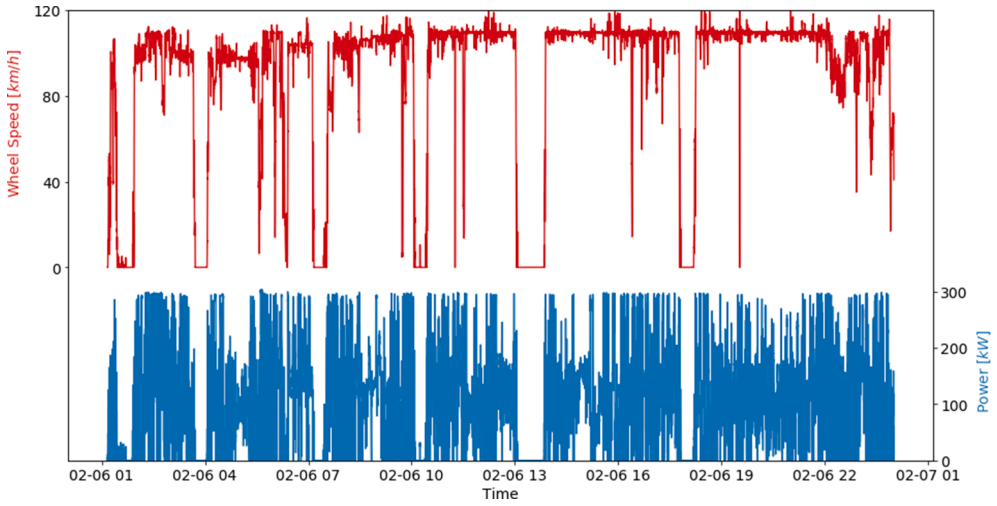

Fig. B.3. Long-haul daily trip with the maximal time duration at high speed.

Regional Haul

- Maximal energy consumption

  Fig. B.4.

- Maximal power-weighted work

  Fig. B.5.

- Maximal time duration at high speed

  Fig. B.6.

- Minimal fuel economy

  Fig. B.7.

Local Delivery

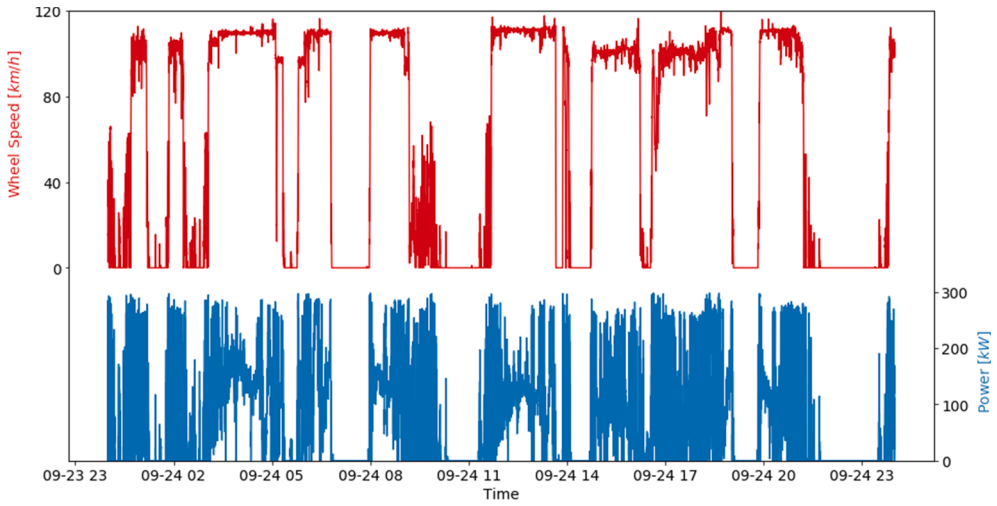

Fig. B.4. Regional-haul daily trip with the maximal energy consumption.

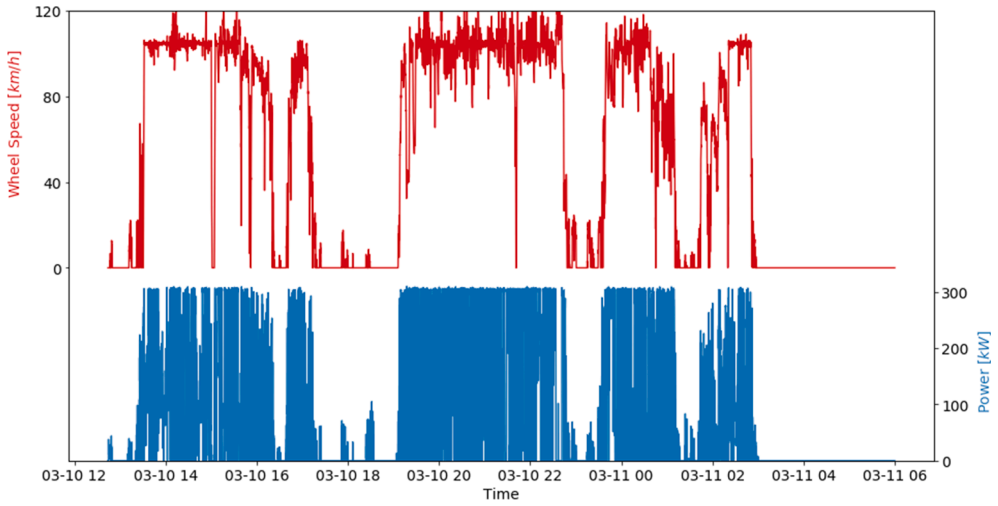

Fig. B.5. Regional-haul daily trip with the maximal power-weighted work.

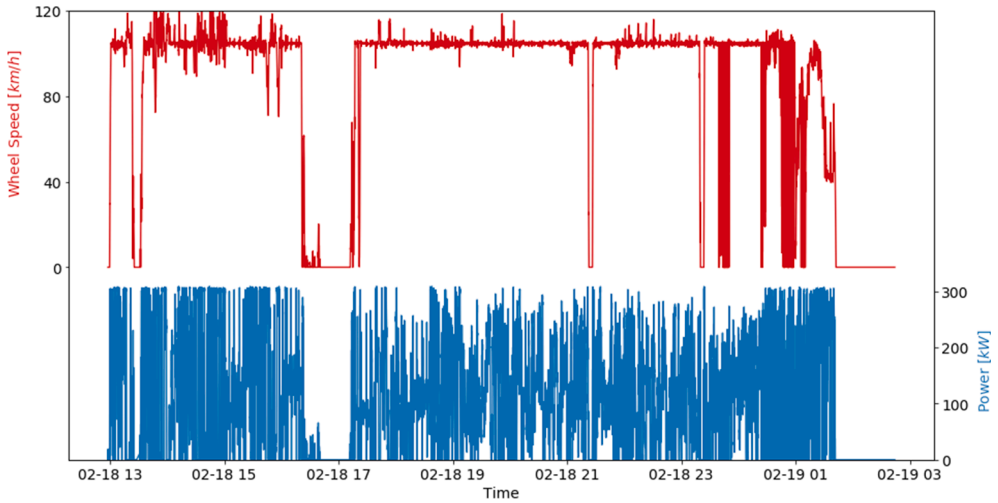

Fig. B.6. Reginal-haul daily trip with the maximal time duration at high speed.

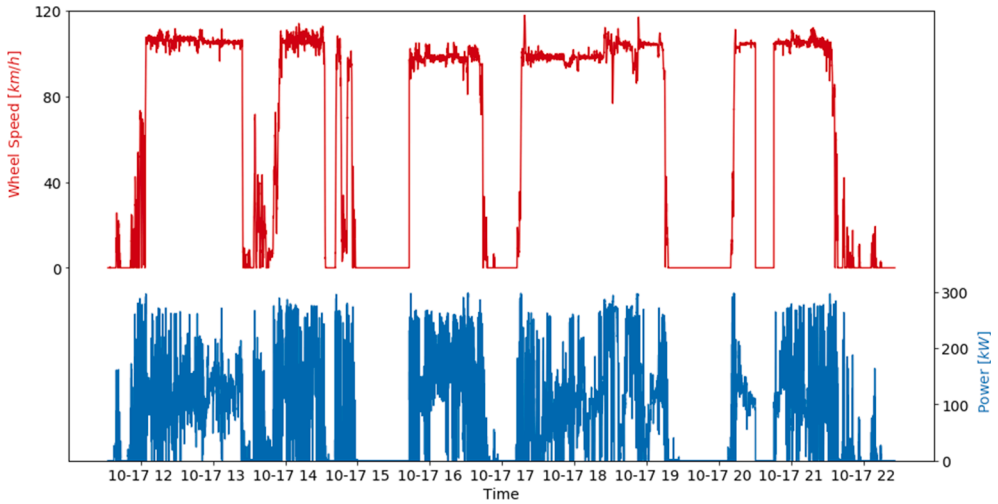

Fig. B.7. Regional-haul daily trip with the minimal fuel economy.

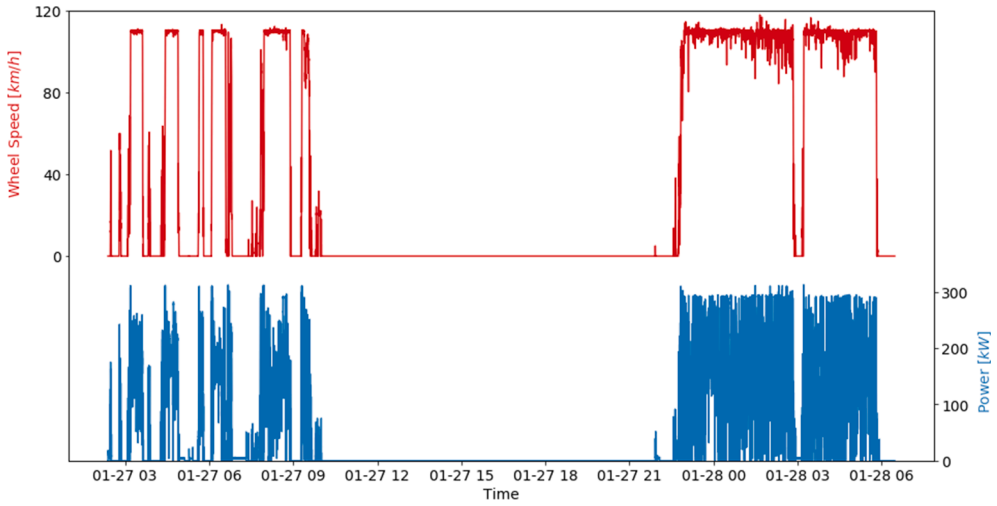

Fig. B.8. Local delivery daily trip with the maximal energy consumption.

- Maximal energy consumption

  Fig. B.8.

- Maximal power-weighted work

  Fig. B.9.

- Maximal time duration at high speed

  Fig. B.10.

- Minimal fuel economy

  Fig. B.11.
  Transit Bus

- Maximal energy consumption

  Fig. B.12.

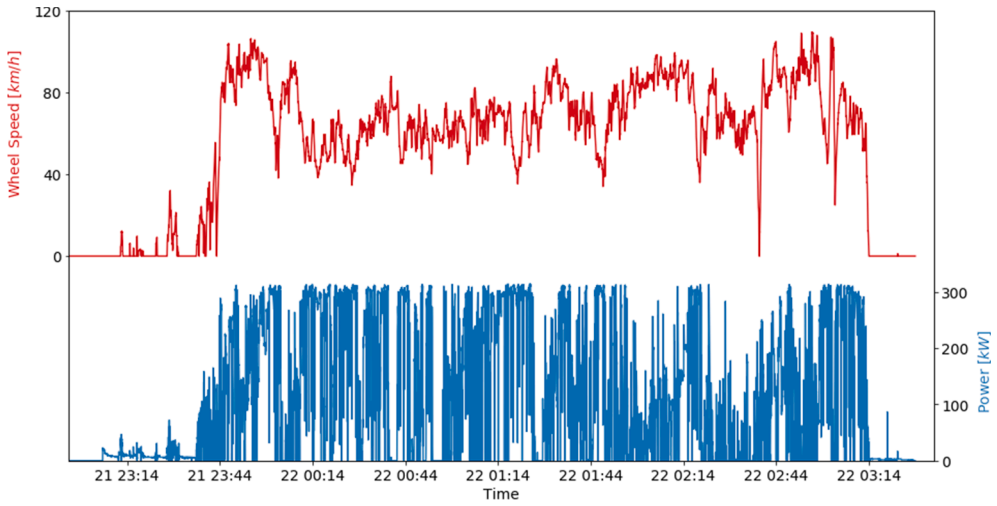

Fig. B.9. Local delivery daily trip with the maximal power-weighted work.

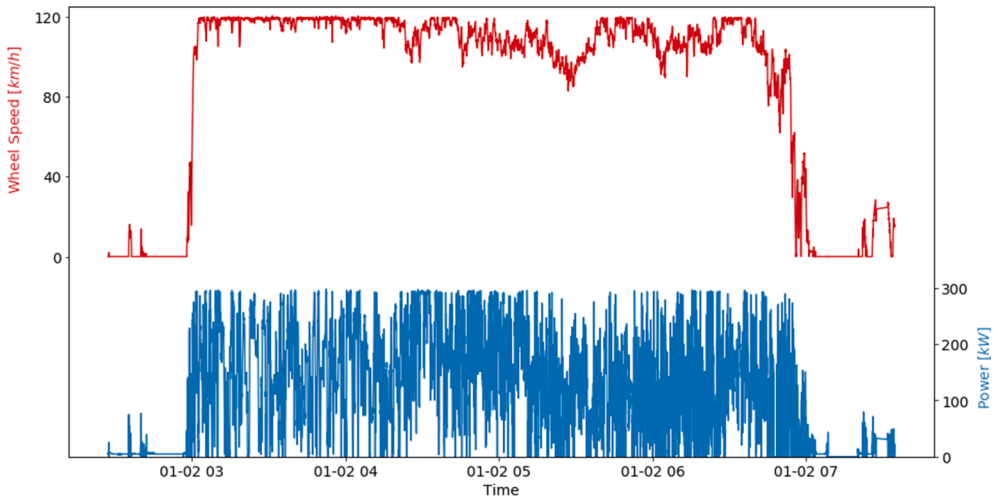

Fig. B.10. Local delivery daily trip with the maximal time duration at high speed.

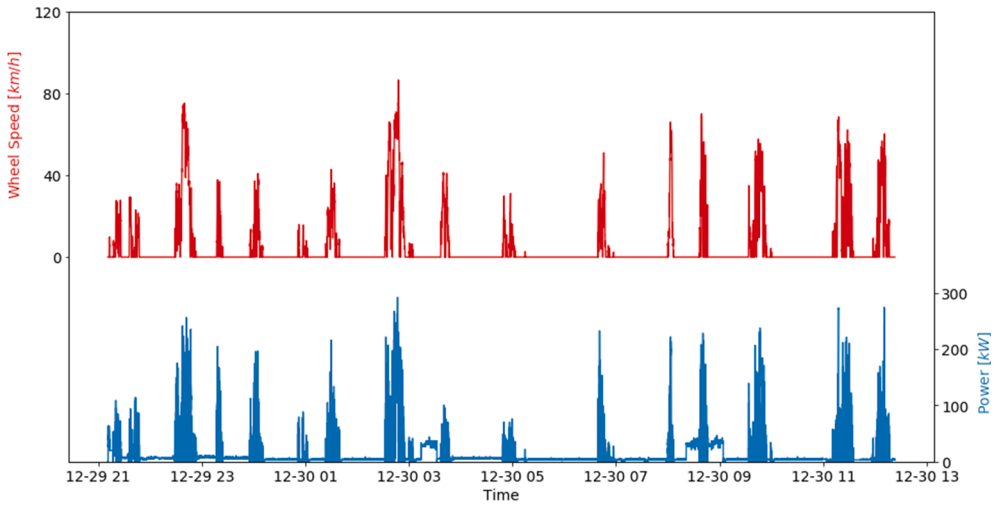

Fig. B.11. Local delivery daily trip with the minimal fuel economy.

- Maximal power-weighted work

  Fig. B.13.

- Maximal time duration at high speed

  Same as maximal power-weighted cycle in transit bus vocation

- Minimal fuel economy

  Fig. B.14.

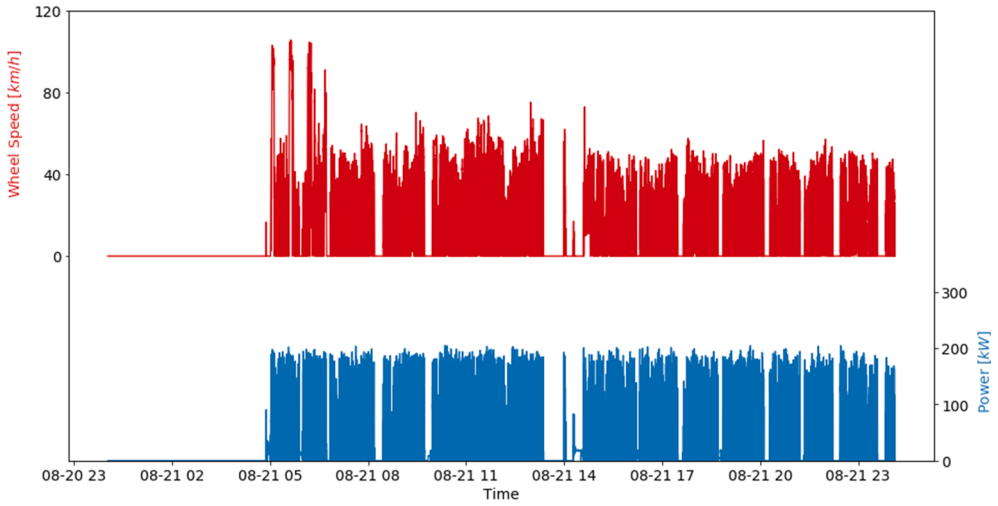

Fig. B.12. Transit bus daily trip with the maximal energy consumption.

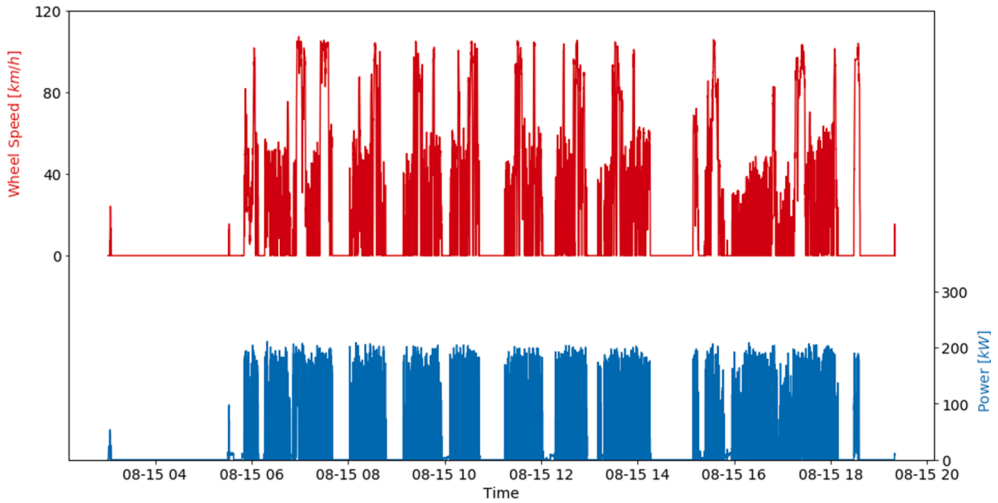

Fig. B.13. Transit bus daily trip with the maximal power-weighted work.

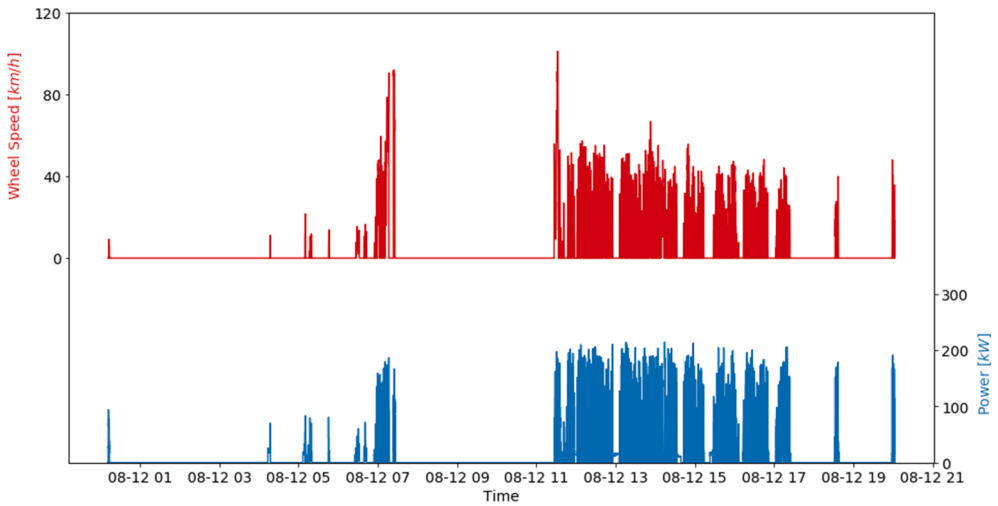

Fig. B.14. Transit bus daily trip with the minimal fuel economy.

References

AB Volvo, 2018. Premiere for Volvo Trucks' first all-electric trucks, https://www.volvogroup.com/en-en/news/2018/apr/news-2879838.html; April 12, 2018.

Amirjamshidi, G., Roorda, M.J., 2015. Development of simulated driving cycles for light, medium and heavy duty trucks: case of the Toronto Waterfront area. Transp. Res. Part D 34, 255–266.

Andre, M., 1996. Driving Cycles Development: Characterization of the Methods. SAE Technical Paper 961112.

Austin, T.C., DiGenova, F.J., Carlson, T.R., Joy, R.W., Gianolini, K.A., Lee, J.M., 1993. Characterization of Driving Patterns and Emissions from Light-Duty Vehicles in California. California Air Resources Board, Final Report, contract no. A932-185.

Brady, J., O'Mahony, M., 2016. Development of a driving cycle to evaluate the energy economy of electric vehicles in urban areas. Appl. Energy 177, 165–178.

California Air Resources Board, 2021. Advanced Clean Trucks, https://ww2.arb.ca.gov/our-work/programs/advanced-clean-trucks?utm_medium=email&utm_source=govdelivery [accessed 11 January 2021].

Daimler, 2021. eActros goes into customer operation, https://www.daimler.com/products/trucks/mercedes-benz/eactros.html [accessed 11 January 2021].

Davis, S.C., Boundy, R.G., 2019. Transportation Energy Data Book: Edition 37. Oak Ridge, TN: Oak Ridge National Laboratory, ORNL/TM-2018/987.

Davis, S.C., Boundy, R.G., 2020. Transportation Energy Data Book: Edition 38. Oak Ridge National Laboratory, Oak Ridge, TN.

Duran, A., Li, K., Kresse, J., Kelly, K., 2018. Development of 80- and 100- mile work day cycles representative of commercial pickup and delivery operation. SAE Technical Paper 2018-01-1192.

Esteves-Booth, A., Muneer, T., Kirby, H., Kubie, J., Hunter, J., 2001. The measurement of vehicular driving cycle within the city of Edinburgh. Transport. Res. Part D: Transp. Environ. 6 (3), 209–220.

Eudy, L., Post, M., 2018. Fuel Cell Buses in U.S. Transit Fleets: Current Status 2018. Golden, CO: National Renewable Energy Laboratory, NREL/TP-5400-72208, https://www.nrel.gov/docs/fy19osti/72208.pdf.

European Commission, 2021. Vehicle Energy Consumption calculation TOol – VECTO, https://ec.europa.eu/clima/policies/transport/vehicles/vecto_en [accessed 11 January 2021].

Fotouhi, A., Montazeri-Gh, M., 2013. Tehran driving cycle development using the K-mean clustering. Scientia Iranica A 20 (2), 286–293.

Gunther, R., Wenzel, T., Wegner, M., Rettig, R., 2017. Big data driven dynamic driving cycle development for busses in urban public transportation. Transp. Res. Part D 51, 276–289.

Ho, S.H., Wong, Y.D., Chang, V.W.C., 2014. Development Singapore driving cycle for passenger cars to estimate fuel consumption and vehicular emissions. Atmos. Environ. 97, 353–362.

Hung, W.T., Tong, H.Y., Lee, C.P., Ha, K., Pao, L.Y., 2007. Development of a practical driving cycle construction methodology: a case study in Hong Kong. Transport. Res. Part D: Transp. Environ. 12, 115–128.

Hyundai, 2018. Hyundai and H2 Energy to launch world's first fleet of Fuel Cell Truck, https://www.hyundai.news/eu/technology/hyundai-motor-and-h2-energy-will-bring-the-worlds-first-fleet-of-fuel-cell-electric-truck-into-commercial-operation; September 19, 2018.

Kamble, S.H., Mathew, T.V., Sharma, G.K., 2009. Development of real-world driving cycle: case study of Pune, India. Transport. Res. Part D 14, 132–140.

Lin, J., Niemeier, D.A., 2002. An Exploratory Analysis Comparing a Stochastic Driving Cycle to California's Regulatory Cycle. Atmos. Environ. 36, 5759–5770.

Mihelic, R., Roeth, M., 2019. More Regional Haul: An Opportunity for Trucking? https://nacfe.org/regional-haul/; April 8, 2019 [accessed 14 February 2020].

National Renewable Energy Laboratory, 2021. Fleet DNA: Commercial Fleet Vehicle Operating Data, http://www.nrel.gov/fleetdna [accessed 11 January 2021].

O'Dell, J., 2018. Here's How Toyota Improved Project Portal, its Fuel Cell Truck, https://www.trucks.com/2018/07/30/toyota-fuel-cell-truck-improvements/; July 30, 2018.

O'Keefe, M.P., Simpson, A., Kelly, K.J., Pedersen, D.S., 2007. Duty Cycle Characterization and Evaluation Towards Heavy Hybrid Vehicle Applications. SAE Tech. Pap. 2007-01-0302, 2007. doi: 10.4271/ 2007-01-0302.

Prohaska, R., Konan, A., Kelly, K., Lammert, M., 2016. Heavy-duty vehicle port drayage drive cycle characterization and development. SAE Int. J. Commer. Veh. 9 (2) https://doi.org/10.4271/2016-01-8135.

Rokach, L., Maimon, O., 2008. Data Mining with Decision Trees: Theory and Applications. World Scientific Pub Co.

Seers, P., Nachin, G., Glaus, M., 2015. Development of two driving cycles for utility vehicles. Transp. Res. Part D 41, 377–385.

Shi, S., Lin, N., Zhang, Y., Cheng, J., Huang, C., Liu, L., Lu, B., 2016. Research in Markov property analysis of driving cycle and its application. Transport. Res. Part D: Transp. Environ. 47, 171–181.

Sun, R., Tian, Y., Zhang, H., Yue, R., Lv, B., Chen, J., 2019. Data-driven synthetic optimization method for driving cycle development. IEEE Access. https://doi.org/10.1109/ACCESS.2019.2950169.

Tesla, 2021. Semi, https://www.tesla.com/semi [accessed 11 January 2021].

Tzirakis, E., Pitsas, K., Zannikos, F., Stournas, S., 2006. Vehicle emissions and driving cycles: comparison of the Athens driving cycle (ADC) with ECE-15 and European driving cycle (EDC). Global NEST 8 (3), 282–290.

U.S. Energy Information Administration, 2020. Annual Energy Outlook 2020. Washington, D.C.: EIA.

U.S. Environmental Protection Agency, 2020. Cleaner Trucks Initiative, https://www.epa.gov/regulations-emissions-vehicles-and-engines/cleaner-trucks-initiative [accessed 11 January 2021].

U.S. Environmental Protection Agency, 2020. Final Rule for Phase 2 Greenhouse Gas Emissions Standards and Fuel Efficiency Standards for Medium- and Heavy-Duty Engines and Vehicle, https://www.epa.gov/regulations-emissions-vehicles-and-engines/final-rule-phase-2-greenhouse-gas-emissions-standards-and [accessed 11 January 2021].

U.S. Environmental Protection Agency, 2020. Sources of Greenhous Gas Emissions, https://www.epa.gov/ghgemissions/sources-greenhouse-gas-emissions [accessed 11 January 2021].

Zhang, C., Sun, Z., 2017. Trajectory-based combustion control for renewable fuels in free piston engine. Appl. Energy 187, 72–83. https://doi.org/10.1016/j.apenergy.2016.11.045.

Zhao, X., Yu, Q., Ma, J., Wu, Y., Yu, M., Ye, Y., 2018. Development of A representative EV urban driving cycle based on A K-means and SVM hybrid clustering algorithm. J. Adv. Transport. 2018, 1890753.